Science of the Total Environment 622–623 (2018) 1363–1378

Contents lists available at ScienceDirect

Science of the Total Environment

journal homepage: www.elsevier.com/locate/scitotenv

Bridging the gap between terrestrial, riverine and limnological research: Application of a model chain to a mesotrophic lake in North America

J. Crossman [a,*], J.A. Elliott [b]

[a] Chemistry Department, Trent University, 1600 West Bank Drive, Peterborough, Ontario K9J 0G2, Canada
[b] Lake Ecosystems Group, Centre for Ecology & Hydrology, Lancaster Environment Centre, Library Avenue, Bailrigg, Lancaster LA1 4AP, UK

HIGHLIGHTS

- We developed a catchment-lake model chain to connect catchment drivers and lake responses.
- High temperatures and low inflows explained most lake low dissolved oxygen events.
- The significance of chlorophyll-*a* was weaker, and depth dependent.
- Warmer, drier summers will likely have a negative impact on lake health.
- Nutrient loads should be reduced by reducing concentrations but preserving flow.

GRAPHICAL ABSTRACT

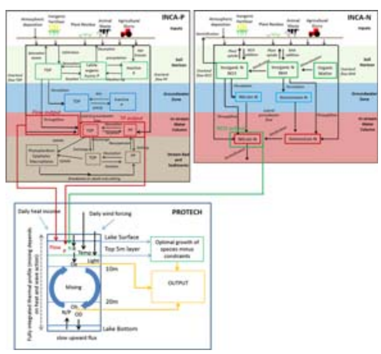

ARTICLE INFO

Article history:
Received 23 June 2017
Received in revised form 4 December 2017
Accepted 4 December 2017
Available online xxxx

Editor: R Ludwig

Keywords:
Dissolved oxygen
Chlorophyll-*a*
Phosphorus
Flow
Temperature
Biochemical oxygen demand

ABSTRACT

Models remain our best available tool for managing low lake dissolved oxygen concentrations, which pose a serious ecological risk. This study investigated whether process-based catchment models (INCA-N and INCA-P) could accurately drive a lake model (PROTECH), to bridge a gap between terrestrial, riverine and limnological research. INCA was calibrated over all 20 catchments of the Simcoe watershed, Canada. Daily outputs (flow, nitrogen and phosphorus concentrations) over the period 2010–2016 were selected for a common “baseline” period, and used as inputs to PROTECH, which was calibrated across the three major basins of lake Simcoe; Kempenfelt (K42), Cooks (C9), and the main basin (E51). Results showed that at catchment outflows INCA models achieved an average flow R^2 of 0.8; a load R^2 of 0.7 (both for TP and N-NO3), a concentration R^2 of 0.4 and 0.5 (for TP and N-NO3 respectively), and an SiO_2 $R^2 > 0.8$. In each basin PROTECH achieved an R^2 for both temperature and dissolved oxygen (DO) concentrations of >0.9. Performance of N-NO_3, TP and Chlorophyll-*a* concentrations were good (R^2 values of up to 0.98, 0.92 and 0.53 respectively). Multi-stressor analyses established that most occurrences when DO dropped below the desired 7 mg/l threshold (DO7) were attributable to combinations of high temperatures and low tributary inflows. The importance of additional drivers was depth dependent, with photosynthesis being particularly important in shallower C9 and E51 basins during summer, when algae contributed sufficient O_2 to the water column to inhibit DO7 events. Conversely in the deeper more strongly stratified K42 basin, greater algal growth boosted the biochemical oxygen demand, enhancing declines in DO. Lake physics explained a significant number of DO7 events in all three basins. Integrated catchment-lake modelling approaches are important in understanding lake physical and ecological processes, and the impacts of land management and future climate change.

* Corresponding author at: Earth and Environmental Sciences, University of Windsor, Windsor, Ontario N9B 3P4, Canada.
E-mail address: jill.crossman@uwindsor.ca (J. Crossman).

https://doi.org/10.1016/j.scitotenv.2017.12.052
0048-9697/

1. Introduction

Low dissolved oxygen (DO) levels are a major concern in many major large water bodies, where DO declines have been attributed to intensified algal growth and decay, originating from increases in nutrient influxes (Diaz, 2001). Studies have shown that reduced DO levels in lake waters affect many biological and ecological processes (Cooper and Washburn, 1949; Breitburg et al., 1997); for instance the population numbers of cold-water fish may decline due to associated negative impacts on fish respiration rates, reproductive activity, and forced changes in habitat location (Kramer, 1987).

Watershed management strategies are often introduced in an attempt to reduce nutrient loads received by lakes. Since the 1980s management efforts including improvements in sewage treatment facilities, have helped to reduce nutrient loads dramatically in many large waterbodies throughout North America and the world (Kaas et al., 1996; Conley, 2000). Initially these efforts were successful in controlling eutrophication, for example in Lake Erie and Lake Simcoe, Ontario, Canada (Watson et al., 2016). Despite reductions in nutrient inputs however, desired lake DO concentrations have not consistently been achieved (Eimers et al., 2005; Burns et al., 2005), and in many watersheds eutrophic conditions have since reoccurred (Sharpley et al., 2012; Reckhow et al., 2011). Their recurrence has in part been linked to complex interactions between land management, terrestrial nutrient transport pathways, and climate change (Smith et al., 2015), and a solution to this pressing water quality issue has not yet been found.

This study looks to further our understanding of the interactions between terrestrial, riverine and limnological nutrient transport and ecological responses through the application of a modelling tool which links two otherwise disparate disciplines (limnology and catchment hydrology). Through this unique basin-wide application of a process-based model chain, with a fine scale spatial and temporal resolution, we hope to establish a more integrated approach to eutrophication studies, which will aid with the development of novel, more resilient management strategies of lakes and their catchments in the face of future change. To demonstrate the importance of connecting these environmental disciplines, we have selected the watershed of Lake Simcoe. This is a large mesotrophic lake in southern Ontario, Canada, in which low DO levels have been a concern since the 1970s (MacLean et al., 1981; Evans et al., 1996; Nicholls, 1997). In the 1990s a variety of nutrient remediation programs were implemented and a critical DO target level of 7 mg/l was set by the Lake Simcoe Protection plan in 2009. Whilst lake DO concentrations have improved since the 1970s, the critical DO targets have not consistently been met, necessitating annual stocking of the local commercial fisheries (Winter et al., 2007).

Two integrated catchment models (INCA-P and INCA-N) are linked with a lake model (PROTECH; Elliott et al., 2010), creating a holistic, process-based catchment-lake simulation of the entire Simcoe basin. Both models operate on a daily timescale, enabling nutrients to be followed from their source, via sub-catchment, terrestrial and aquatic process interactions, through to the lake itself. Within the lake the daily impact of changes in nutrient fluxes upon phytoplankton and DO levels is simulated. Unlike other lake models used throughout Simcoe's history, (Rasmussen and Kalff, 1987; Snodgrass and Holubeshen, 1992; Nicholls, 1997) PROTECH is process-based and capable of receiving multiple daily inputs of nutrients and flow from individual tributaries (from INCA-P and INCA-N). Many previous lake modelling studies have either been empirical (e.g. Snodgrass and Holubeshen (1992) and Nicholls (1997)) and thus not suitable for scenario projections, or have used models specifically designed for management effectiveness analysis, such as SWAT (Neitsch et al., 2011), giving longer term yields, and leaving them unable to project changes in the frequency of shorter events, e.g. daily decreases in DO concentrations. These short events can be biologically important, for example a single occurrence of hypoxia can threaten the capacity of juvenile fish to perform critical daily life support activities (Evans, 2006). The omission of short-term events of high ecological impact could lead to an overestimation of potential ecological improvements. With a direct transition between INCA outputs to PROTECH inputs, the application of this model chain looks to provide key process information on lake responses to catchment inputs. The models used offer a spatial (subcatchment) and temporal (daily) resolution of nutrient and DO interactions not previously explored from source to impact. INCA-PROTECH is hoped to be an ideal model combination as it can provide a high resolution output without exceeding the calibration capacity of the observed (daily) data.

The specific aim of this study was to assess whether the INCA-PROTECH model chain was capable of accurately representing catchment and lake dynamics, to further our understanding of responses of lake DO and ecology to catchment drivers, and to determine if the tool is suitable for assessing the effectiveness of nutrient management strategies in restoring lake health.

2. Methods

2.1. Site description

The Lake Simcoe watershed is located between Lake Ontario and Georgian Bay, with a total terrestrial area of 2899 km^2 (Winter et al., 2011), consisting of around 20 tributary catchments. Most of these tributaries are routinely monitored by either the Lake Simcoe Region Conservation Authority, or Environment Canada, although some inflows have remained ungauged. The lake has a surface area of 722.5 km^2, and consists of a main basin (average depth 14 m) and two large bays, the deeper Kempenfelt Bay to the west (maximum depth 42 m), and the shallower Cook's Bay to the south (maximum depth 15 m). Simcoe has a single outflow through the Atherly Narrows to Georgian Bay via the Trent Severn Waterway.

Quaternary geology varies substantially between the 20 catchments, ranging from a very low clay content in the northwest (<1%) to over 71% in the northeast (Fig. 1). Marked differences in surface overland flow and soil residence times have been attributed at least in part to this spatial variance in catchment geology, where clayey soils and tile drainage have been associated with rapid through flow and high proportions of surface runoff, and sandy loams associated with lower rates of hydrological transport and higher soil water storage capacity (Oni et al., 2014; Crossman et al., 2014).

Agriculture is the dominant landuse in the Simcoe watershed, covering over 50% of the total area, and is generally greatest in the south and east. Lower agricultural activities in the northern and western regions are associated with a series of urban centres, including the cities of Barrie and Orillia. In the Holland catchment, despite the presence of the city of Bradford, extensive farming of polders (drained wetlands) contributes to a catchment agricultural landuse of over 50% (derived from Ecological Land Classification of Ontario data, Ontario Ministry of Natural Resources, 2007).

Temperatures are similar across the watershed, but were generally cooler in the north than in the south, ranging from 6.1 °C at Orillia, to 7.4 °C in the Maskinonge (2006–2015 average, Thornton et al., 2016). The total annual rainfall in Simcoe is 904 mm, although this varies considerably across the watershed. Precipitation in some of the western catchments feeding Kempenfelt Bay is especially low, where sites such as Barrie and Leonard receive only between 596 mm and 663 mm respectively, compared to those in the North and South which receive up to 1046 mm (Hawkestone) and 1029 mm (Black). Snowmelt is a key hydrochemical event within all catchments, evidenced by a spring flow maximum (March–May) which declines throughout summer to seasonal lows occurring in later summer and early fall (September–November) (Crossman et al., 2016). Periods of ice coverage differ considerably between basins, ranging from 90 days in Kempenfelt Bay to 104 days in Cooks' Bay.

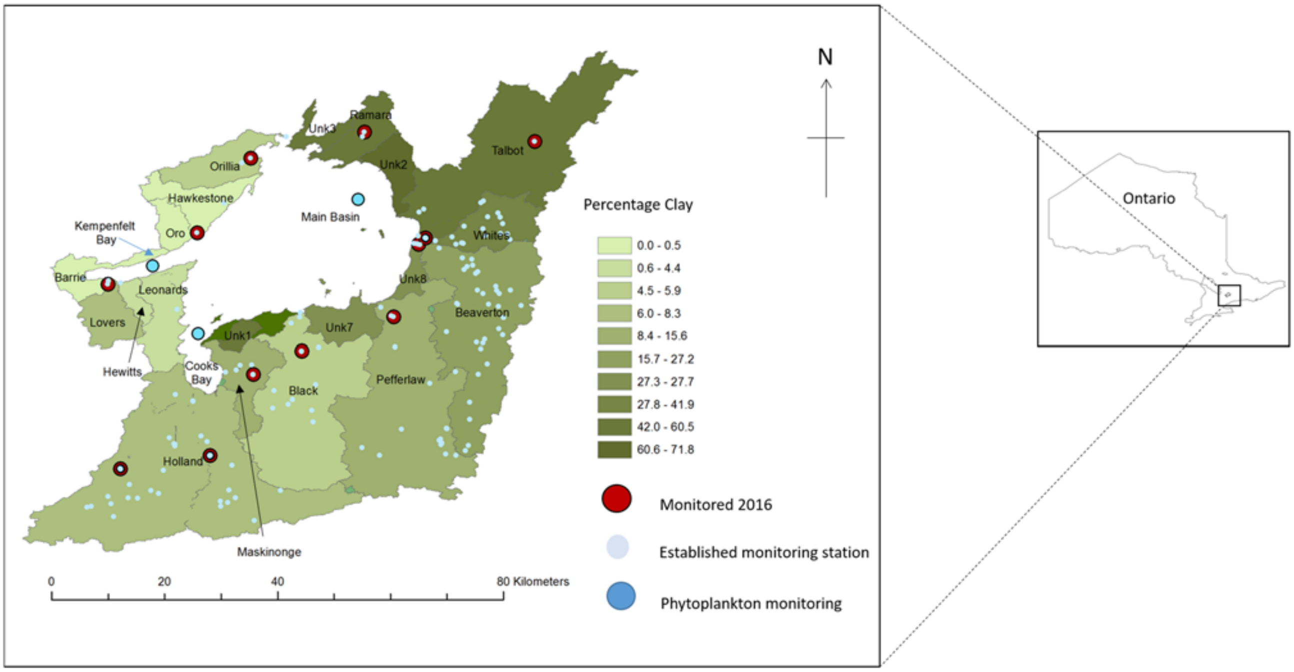

Fig. 1. Soil characteristics of the Simcoe watershed (derived from data available from Soil Landscapes of Canada Working Group, 2010) showing monitoring locations over the 2015–2016 field period with historical monitoring stations indicated in light blue. (For interpretation of the references to color in this figure legend, the reader is referred to the web version of this article.)

2.2. Monitoring

Routine monitoring programs within the Simcoe watershed typically consist of samples collected on a twice-monthly basis, which can lead to misrepresentations of annual nutrient loads (O'Connor et al., 2013). This low resolution also creates difficulties in achieving high model precision during key hydrochemical events. In 2016 a basin-wide, single season, high frequency event-sampling regime was implemented in order to help fill perceived gaps in observed data, enhance process understanding, and give an improved basis for comparison to modelled data. In addition, to extend the spatial extent of load estimations around the watershed, a low frequency sampling program was implemented from August 2015 to June 2016 which included previously unmonitored basins.

Flow gauges were installed in August 2015, at the outflows of the Oro, Orillia, Beaver and Pefferlaw tributaries. The Talbot, which has been heavily modified, was monitored at the downstream extent of its natural flow regime, and the Ramara was monitored as far downstream as could be accessed through public lands (Fig. 1). Water quality samples were taken twice a month until ice break-up in 2016, and DO and water temperature were measured on site. Samples taken were analysed for N-NO_3, NH4, TP, DP, PP, SiO_2, and Chl-*a* using standard MOECC analytical methods (Janhurst, 1998). During spring 2016, water quality samples were taken twice weekly (~every 3 days). This high frequency program was applied at the 6 previously unmonitored stations in the north, and at 6 established stations in the south (Fig. 1). The established stations were chosen for the length of their long term flow records, and their proximity to catchment outflow. Samples were also taken daily at three of the stations (HLD1, HLD2 and WHT) using automated ISCO samplers.

High frequency samples (twice weekly) were also taken from three sites within the lake itself. The chosen lake sites represent the three main basins (Kempenfelt Bay, Cook's Bay and the main lake), and were selected to complement existing low frequency monitoring programs of LSRCA and the MOECC. Lake samples were collected with a PVC hose, as composites through the euphotic zone where the lower depth was determined as 2.5 times the Secchi disk depth, up to a maximum depth of 15 m (Winter et al., 2011). These samples were analysed for N-NO_3, NH_4, TP, DP, PP, SiO_2, Chl-*a* and phytoplankton species abundance and biomass. Dissolved oxygen and thermal profiles were also conducted on each sampling occasion.

2.3. Modelling

A model-chain was set up between two semi-distributed catchment models (INCA-N and INCA-P), a daily SiO_2 model, and a series of Lake models (PROTECH). The INCA models were used to calculate transport of water, sediment and nutrients (Nitrogen and Phosphorus) in both the terrestrial and aquatic phase, throughout the 20 tributary catchments of the Simcoe watershed. Daily outputs from the SiO_2 and INCA models were used as driving inputs to three PROTECH models which were set up to represent the primary basins of Lake Simcoe (Kempenfelt, Cooks and the main basin) (Fig. 2). The bays of Kempenfelt and Cooks received external inputs supplied by INCA and the SiO_2 models; however the main basin additionally received inflows from the two lake basins (supplied by PROTECH) (Fig. 3). This model chain structure helped to support high spatial resolution throughout the study.

2.3.1. INCA model

Both INCA-N (version no. 1.0.16) and INCA-P (version no. 1.4.12) use a daily time series of precipitation and temperature data, which was taken from the Daymet daily surface weather data (Thornton et al., 2016). The models also require a daily input series of hydrologically effective rainfall (HER) and soil moisture deficit (SMD), which was generated using an external rainfall-runoff model, PERSIST, for each of the 20 catchments. PERSIST is a watershed-scale hydrological model developed specifically for INCA applications (Futter et al., 2014). Each INCA model application was calibrated using a combination of field measurements, GIS data, literature values, expert judgement and statistical analysis. Calibration periods were selected for each catchment which reflected the maximum available period of observed data (Crossman et al., 2016). The calibration method, as is standard with catchment models, was to assume that each concentration and flow observation

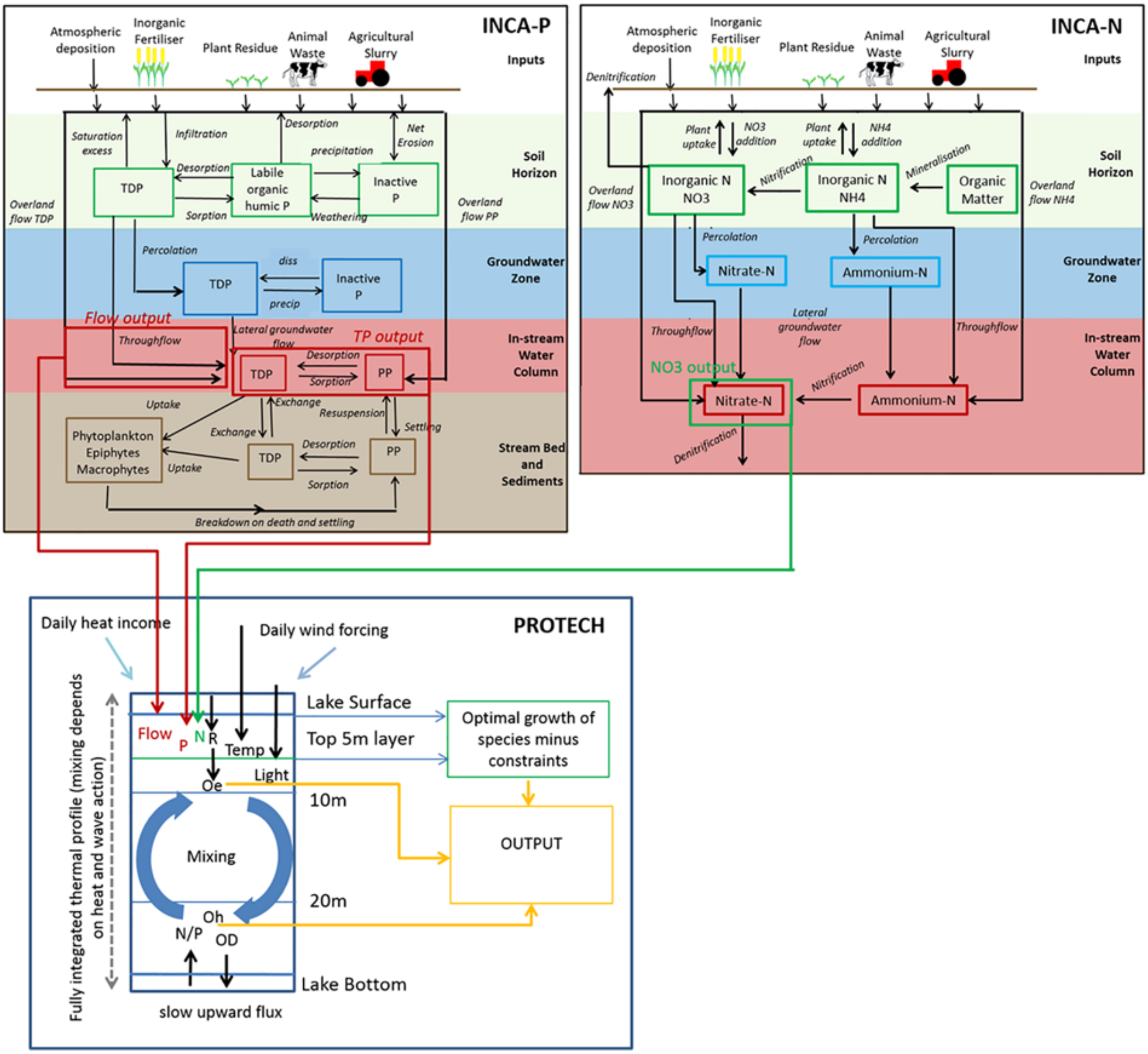

Fig. 2. Conceptual figure of INCA-PROTECH model chain.

had equal value and to calibrate to each of them. Additional validation was performed for 9 models over the 2015–2016 period, using the high frequency monitoring data collected during the program. A hydrological network was developed for each study catchment, using a digital elevation model within ArcHydro GIS software. 5 classes of landuse were initially used based on data obtained from the Ecological Land Classification of Ontario Data (Ontario Ministry of Natural Resources, 2007), including urban, intensive agriculture, nonintensive agriculture, wetlands and forest (SI1).

Direct nutrient additions to the Simcoe catchments include fertiliser applications, sewage works, septic systems, stormwater outflows, and atmospheric deposition (Fig. 2). Rates of nitrogen and phosphorus fertiliser additions from crops were calculated for both intensive and nonintensive agricultural areas using a combination of local recommended nutrient application rates (OMAFRA, 2009), and reported crop growth statistics (Statistics Canada, 2011a). Nutrient inputs from livestock were calculated using reported herd numbers, combined with Ontario livestock nutrient coefficients. Application rates were applied over a 60 day period to intensively farmed areas, and a 120 day period to nonintensive agricultural areas, beginning in late April. Nutrient inputs from sewage treatment plants were determined from data provided by XCG consultants, and KMK consultants. Atmospheric deposition of P and N were taken from monitoring data reported in Ramwekellan et al. (2009), and from LSRCA monitoring data (unpublished data, 2017).

In addition, groundwater nutrient concentrations were calibrated using data provided by the Provincial Groundwater Monitoring Network (2012), and initial soil P concentrations calculated from values measured by Fournier et al. (1994). Soil equilibrium coefficients were based on laboratory-derived equilibrium phosphorus concentrations (EPCo) and Freundlich Isotherm values calculated for different landuse and soil types (Peltouvouri, 2006; Väänänen, 2008; Koski–Vähälä, 2001).

A complicating factor in the calibration of the INCA models is the historic implementation of management strategies; previous work has established that these have had a significant impact on nutrient loads over time (Crossman et al., 2016). It was therefore important to include some of these temporal changes in the calibration period, which include the restriction of livestock access to watercourses, upgrading of malfunctioning septic systems and retrofitting of urban ponds. Methods of calculation for nutrient input timeseries have been discussed elsewhere (Crossman et al., 2016) although a summary is provided here.

A timeseries representing the impacts of restricting livestock access to watercourses was calculated, using livestock access data, and nutrient load inputs per animal (based on monitoring data from Crossman et al., 2016). In combination with records of dates and sites of management

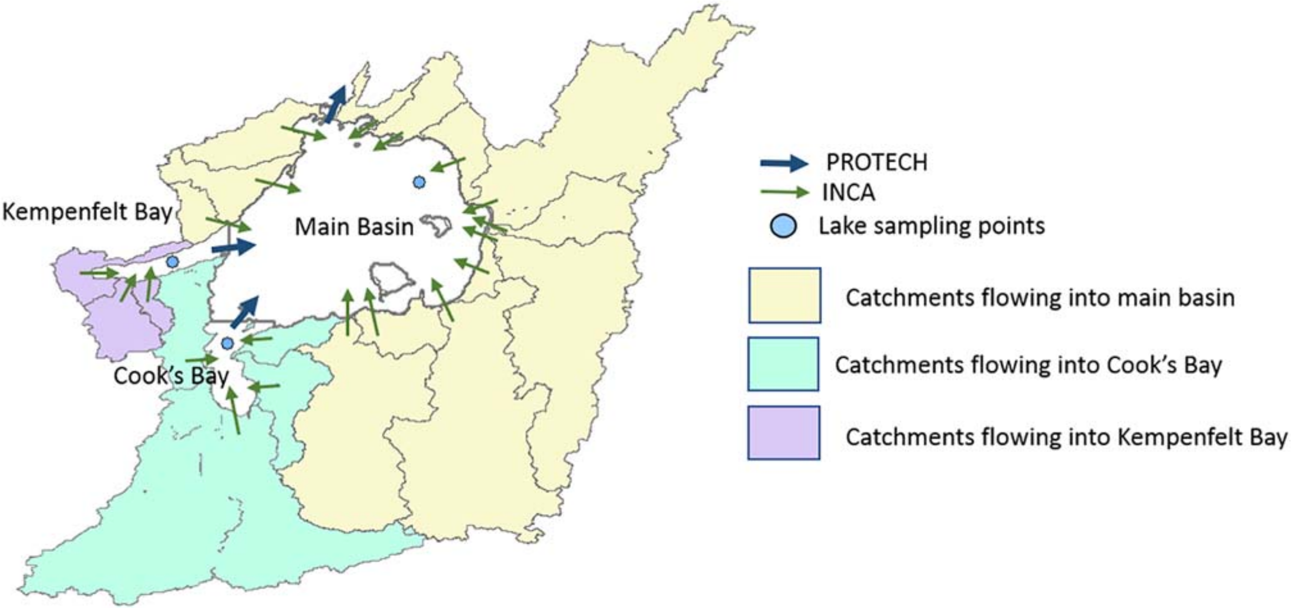

Fig. 3. Assignment of INCA modelled catchments to PROTECH modelled lake basins.

implementation from the Landowner Environmental Assistance Program (LEAP) provided from the LSRCA, this enabled the construction of a site-specific daily time series of N and P inputs from livestock access, which decreased as management plans were applied.

$$\mathrm{LTID} = \mathrm{LSA} \times \mathrm{LRA} \tag{1}$$

where LTID is the daily livestock input of nutrients for the INCA model (kg/day), LSA is the number of livestock with direct access to a water course, and LRA is the nutrient loading rate per animal (kg/animal/day).

A timeseries of input loads from septic systems was also calculated for each subcatchment, using the average nutrient load from excretion (2.6 g TP and 18 g N per person per day; Stephens, 2007), household population numbers, and the number of households connected to septic systems (Louis Berger Group Inc., 2010). The LEAP specifies that funding will be allocated for upgrades only where septic systems are malfunctioning, or where they are located within 100 m of a watercourse (i.e. where nutrients are leaking directly into rivers (May et al., 2011)). It is assumed here that systems which have not been upgraded are not malfunctioning. For each subcatchment, nutrient loads from septic systems which had not been addressed by management strategies under the LEAP were added directly to soils, using the following equations for both seasonal and permanent dwellings.

$$\mathrm{TSI} = \mathrm{HA} \times (\mathrm{HHS} - \mathrm{HHM}) \times \mathrm{H\%} \times \mathrm{PI} \times \mathrm{DY} \times \mathrm{PIP} \tag{2}$$

where TSI is the terrestrial septic input (kg/yr), HHS is the number of households connected to septic systems, HA is the average number of people in a household, HHM is the number of households upgraded through management strategies, H% is the percentage of households as registered residences (as a proportion of permanent or seasonal (cottages) residences), PI is the nutrient input load per day (Kg/day) and DY is days residing in the household (80 for temporary residences, 365 for permanent), and PIP is the proportion of nutrient load released from the soils. The values for both seasonal and permanent septic systems were then summed, added to the "non-intensive" agricultural fertiliser values, and input to the INCA model as a daily time series.

$$\mathrm{NI} = \left(\frac{\mathrm{FI}}{120}\right) + \left(\frac{\mathrm{TSI}}{120}\right) \tag{3}$$

where NI is nutrient input to non-intensive agricultural areas (kg/day), and FI is fertiliser input calculated from crops and livestock (kg/year). Loads from malfunctioning systems were added directly to the river as:

$$\mathrm{SSIM} = \mathrm{HHM} \times \mathrm{HA} \times \mathrm{PI} \times \mathrm{DY} \tag{4}$$

where SSIM is the stream septic input from malfunctioning systems. The variable HHM was updated with every upgrade reported by the LEAP, generating a time series where a registered septic upgrade was simulated by removal of nutrient loads from the stream, which was instead applied to soils with the assumption of a 57% P removal efficiency, and 15% N removal efficiency.

Finally, phosphorus inputs from stormwater drains and urban ponds were calculated for each subcatchment within the INCA-P model using data provided on nutrient concentrations of inlet and outlets from the LSRCA, and simulated urban runoff data from the INCA-P model.

$$\mathrm{StO} = \frac{(\mathrm{Sc} \times 1000) \times (\mathrm{Sn} \times \mathrm{Sf})}{(1000 \times 1000)} \tag{5}$$

where StO is stormwater outlet phosphorus loads (kg/year), Sc is stormwater outlet phosphorus concentration, Sn is the number of stormwater outlets in the subcatchment, and Sf is the total simulated flow per outlet (m^3/year).

$$\mathrm{StP} = \frac{(\mathrm{SpC} \times 1000) \times (\mathrm{SPn} \times \mathrm{SPf})}{(1000 \times 1000)} \tag{6}$$

where StP is the phosphorus loads from stormwater ponds (kg/year), SPc is the P concentration in stormwater pond outlets (mg/l), SPn is the number of stormwater ponds, and SPf is the simulated flow per pond (m^3/year). The StO and StP loads are summed as the total P load from urban stormwater inputs:

$$\mathrm{USI} = \mathrm{StP} + \mathrm{StO} \tag{7}$$

where USI is the total P load from urban stormwater inputs (kg/year). Retrofitting during 2004–2016 was calculated using data from the LSRCA, of an average concentration reduction of 0.134 mg/l P per pond.

$$\mathrm{PR} = \frac{(\mathrm{Sprc} \times 1000) \times (\mathrm{SPRn} \times \mathrm{SPf})}{(1000 \times 1000)} \tag{8}$$

where PR is the reduction in P input (kg/year) resulting from retrofitting ponds, SPrc is the reduction of P concentration in stormwater output ponds (mg/l), and SPRn is the number of stormwater pond reduction strategies implemented. These annual values were removed from USI, to generate a time series of urban nutrient loads which take account of pond retrofitting:

$$\mathrm{UNL} = \mathrm{USI} - \mathrm{PR} \tag{9}$$

where UNL is urban nutrient loads (kg/year).

Loads of N and P from river outflows of all 20 catchments were calculated for the period 2010 to 2016. In each instance the model was actually run from 1985 to 2016 in order to enable stabilisation of any long term processes (e.g. of soil labile P).

2.3.2. Silica model

In addition to flow, N and P inputs, PROTECH requires a daily flux of SiO_2 from each tributary. As such high resolution data is not available in Simcoe, a model was developed to generate the information. A generalised linear model was applied across the watershed, using observed SiO_2 concentrations, river discharge, soil moisture deficit, catchment area and season.

Once calibrated, the model was applied to all 20 catchments of Simcoe, using quaternary geology (Agriculture and Agri-Food Canada, 2010), and the same SMD and flow values from the INCA models. The resultant daily outputs from the SiO_2, INCA N and INCA P models were used as inputs for the PROTECH models.

2.3.3. PROTECH

PROTECH is a process-based spatially explicit model, capable of receiving multiple daily inputs (of nutrients and flow) from individual river networks. The model provides a fully integrated thermal temperature profile, which can simulate the onset of lake warming, thermocline formation, the extent of down-mixing in summer, and eventual collapse of stratification in autumn. It also simulates the slow upward flux of nutrients from high concentrations in the hypolimnion towards the upper mixed layers in the water column. PROTECH uses a basic state variable equation to determine the daily change in Chl-*a* concentrations (X, mg/m^3), which forms the core biological component of all PROTECH model applications (Elliott et al., 2007).

$$\frac{\mathrm{Dx}}{\mathrm{dt}} = \left(\mathrm{r}^{\mathrm{l}} - \mathrm{S} - \mathrm{G} - \mathrm{D}\right)\mathrm{X} \tag{10}$$

where r^l is daily growth rate, S is daily loss due to settling out in the water column, G is daily loss due to grazing, and D is daily loss due to dilution. Changes in the vertical profile are incurred on a daily time-scale, at 10 cm increments, and the extent of mixing (of light, nutrients, and temperature) is based on the Monin-Obukhov length calculation (Imberger, 1985) driven by daily wind speed, cloud cover, time of year and latitude. Most recently, a dissolved oxygen component has been built into PROTECH, based on the LOX model (Bell et al., 2006; Elliott and Bell, 2011). Additional information on model structure and performance can be found in Elliott et al. (2010).

Temperature and precipitation data for the PROTECH calibration were derived from the same gridded source as that used for the PERSiST and INCA models. Windspeed, humidity and cloud cover were taken from the closest available Environment Canada meteorological station for each basin. Lake data including maximum depth, total water volume and surface area were also required, and were derived from a digitised bathymetric map provided by OMNR, which was originally interpreted from depth soundings taken by the Canadian Hydrographic Service (1957).

Inflows from the INCA and SiO_2 models were assigned to each of the three basins according to the hydrological network (Figs. 2 and 3), and the models were calibrated over the 2010–2016 period. Monitoring data used in the calibration were taken from sites K42, C9 and E51, and include water temperature and concentrations of DO, N-NO_3, TP, SiO_2 and Chl-*a*. Ratios of TP:SRP monitored between 1980 and 2008 were used to calculate current lake SRP within each basin (SI2), and to assess the accuracy of PROTECH SRP simulations.

Lake phenological records (timing of ice-on and ice-off) were supplied by the Lake Ice Analysis Group (2012). Data gaps were infilled using detailed descriptions and video-records available on local ice-fishing forums. During ice-on periods, a universal correction was applied to all three PROTECH models consistent with previous PROTECH under-ice applications (e.g. Elliott et al., 2007). This forced lake water temperature to 3.5 °C, reducing incoming light by 50%, and restricting the mixed depth to 0.5 m below the surface. These corrections were designed to simulate the impacts of ice and an inverted thermocline upon phytoplankton (Elliott et al., 2007).

At site K42, internal P loads of 0.03 μg/l were released between July 1st and October 1st (or 1350 kg/year), consistent with LSRCA observations (2005). In addition, densities of zebra mussels which were first identified in Lake Simcoe in 1994, have been projected to be higher at site K42 than in C9 and E51 (Schwalb et al., 2013). To simulate the ability of zebra mussels to reduce phytoplankton biomass (McMahon, 1991) an additional loss rate of 0.02 day^{-1} was added to the baseline grazing rates of the Chl-*a* equation at this site (Eq. 10, parameter G). At site C9, internal P loads of 0.01μg/l were released between July 1st and October 1st. At site E51, where bed sediments have not been identified as a significant long-term source of P, (Dittrich et al., 2013), and low densities of zebra mussels have been identified, no internal P loads or mussel grazing rates were simulated.

2.3.4. Assessment of model accuracy

Model results at multiple locations (river, watershed and lake) were compared to available monitoring data over the period 2010–2016 at daily, seasonal, monthly and annual timescales. Nutrient loads derived from observed data were also compared to those derived from INCA model outputs. As the frequency of in-stream observed chemistry data varied, 'observed' loads were calculated using the midpoint method (Scheider et al., 1978) where an unknown concentration was assumed to be equal to that of the closest sampling date (Casson et al., 2010). Daily stream concentrations were then multiplied by daily stream flow to obtain stream exports. The ability of the models to simulate trends over time was assessed using the coefficient of determination (R^2), and the difference between simulated and actual values expressed using root-mean-square-error (RMSE).

2.3.5. Polynomial analysis

Bowes et al. (2016) have established a methodology for analysis of multiple stressor controls on high frequency monitoring data. These methods are applied to model outputs with the aim of identifying the primary drivers of critically low dissolved oxygen concentration events. First, the daily Chl-*a* and DO concentration model output data were analysed in boxplots (y-axis), with additional model output variables (SRP, N-NO_3, Flow and water temperature) used to investigate potential threshold relationships (x-axis). Multi-stressor relationships identified in these boxplots were then quantified using multiple regression analyses, and displayed in 3-D surface plots.

3. Results

3.1. Model calibrations and validations

Individual subcatchments demonstrated a good fit between monitored flow values and those simulated by INCA, with R^2 values generally above 0.8 (Fig. 4A). In general model performance was greatest in catchment outflows, though there was considerable spatial variability in model performance statistics for TP and N-NO_3 concentrations within each catchment (Fig. 4C,D).

Loads of TP and N-NO_3 were well represented throughout the catchments during the entire calibration period, with R^2 generally above 0.65; and very well represented at the catchment outflow with R^2 above 0.7 (Fig. 4A). The model represented the differences in TP and N-NO_3 concentrations between catchments with R^2 of 0.95 and 0.91 (Fig. 5A,B) and although catchment average N-NO_3 concentrations were typically under-estimated by the simulations (Fig. 5B), loads were generally well represented between catchments with R^2 of 0.67 (TP) and 0.93 (N-NO_3).

Model response to spring freshet was assessed at the sites where high intensity spring melt monitoring was conducted. Comparisons of daily simulated and observed flow, and TP and N-NO_3 concentrations were made during both the rising and falling limbs of the hydrographs, in addition to a comparison of weekly outputs during the entire snowmelt period (e.g. Fig. 6A–D).

Model hydrographs demonstrated a high R^2 with observed flow throughout the snowmelt period (average of 0.83 across the catchments), though daily accuracy was generally higher on the falling (R^2 of 0.78) than the rising limbs (R^2 of 0.47). Conversely, nutrient concentrations were generally more accurately represented during rising limbs, with an average TP R^2 of 0.55 and N-NO_3 R^2 of 0.52 during initiation of snowmelt, compared to an R^2 of 0.27 and 0.28 towards the end of the event. N-NO_3 concentrations were under-predicted by the INCA-N model in most catchments during the spring melt period. A comparison between models applied to different soil types (Fig. 4B) over the snowmelt period demonstrates that although the mean model accuracy for N-NO_3 concentrations was higher in sandy soils (<30% clay) and for TP concentrations was higher in clayey soils (>30% clay), there was no significant difference in model performance between simulations applied in catchments of different soil types.

Across all monitored watersheds, the silica model provided accurate estimations of instream concentrations with an R^2 of 0.64 (daily) (e.g. Fig. 7), 0.8 (annual) and 0.9 (seasonal) (Table 1). Within individual catchments, seasonal and daily R^2 values were predominantly >0.8, though the model fit within the Pefferlaw was less accurate, with a seasonal R^2 of 0.5, and daily R^2 of 0.4.

3.2. Lake simulations (PROTECH)

Between 2010 and 2016, all basins demonstrated an excellent fit between modelled and monitored temperatures within the euphotic zone (Table 2, Fig. 8A), at the seasonal, monthly and annual temporal scale ($R^2 > 0.87$). At the monthly and annual time scale, dissolved oxygen concentrations modelled at the 5 m bottom-zone demonstrated a similarly good fit with observed data ($R^2 > 0.8$) (Table 2, Fig. 8C). The 5 m bottom zone of Lake Simcoe was selected for the focus of the DO study as this has been identified as priority lake trout habitat for juveniles during late summer (Evans et al., 1996). Seasonal correspondences were also excellent at K42 and E51, though slightly lower in basin C9 (R^2 0.31). Despite this, the RMSE remained low (0.4 mg/l) and comparable with the error at other basins.

Basin performance of N-NO_3, TP and Chl-*a* within the euphotic zone was generally excellent at the monthly scale, with R^2 up to 0.98 (N-NO_3), 0.92 (TP) and 0.53 (Chl-*a*) respectively. Associated RMSE was low, between 27.4 μg/l (N-NO_3) and 0.3 μg/l (Chl-*a*). Performance of the model for predicting nutrients and Chl-*a* at seasonal and annual scales was more variable between basins. All basins performed well at the seasonal scale in projecting nutrient concentrations, with an R^2 of up to 0.98 (N-NO_3), and 0.88 (TP). Chl-*a* performance was also high in basins C9 and K42 (R^2 of up to 0.52), though was lower in basin E51 (0.15); RMSE for this variable was exceptionally low however at only 0.2 μg/l. In basin E51, predictions of TP and Chl-*a* were much improved at the annual scale (R^2 of 0.71 and 0.33 respectively). N-NO_3 predictions were less accurate (R^2 0.14), though again RMSE was comparable, at

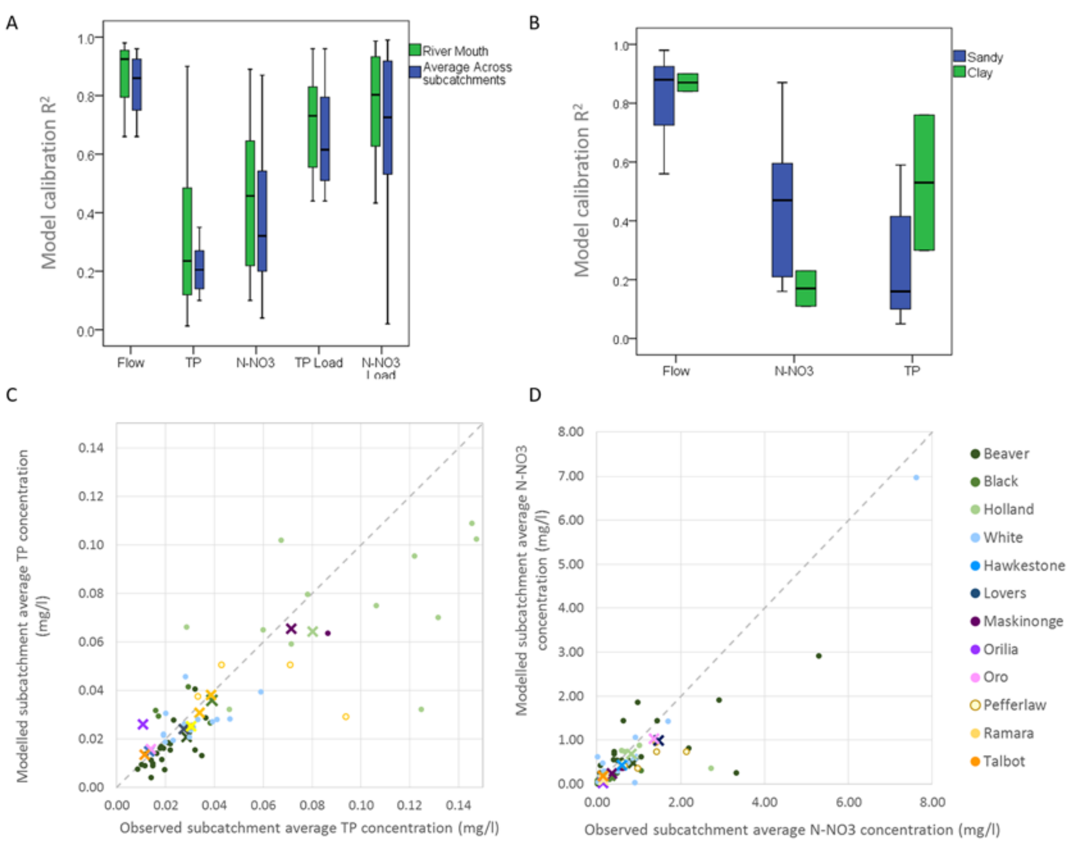

Fig. 4. A) model accuracy statistics over whole calibration period; B) performance statistics during snowmelt (separated by soil type; C) Representation of model performance (TP concentration) by sub catchment; D) Representation of model performance (N-NO_3 concentration) by sub-catchment.

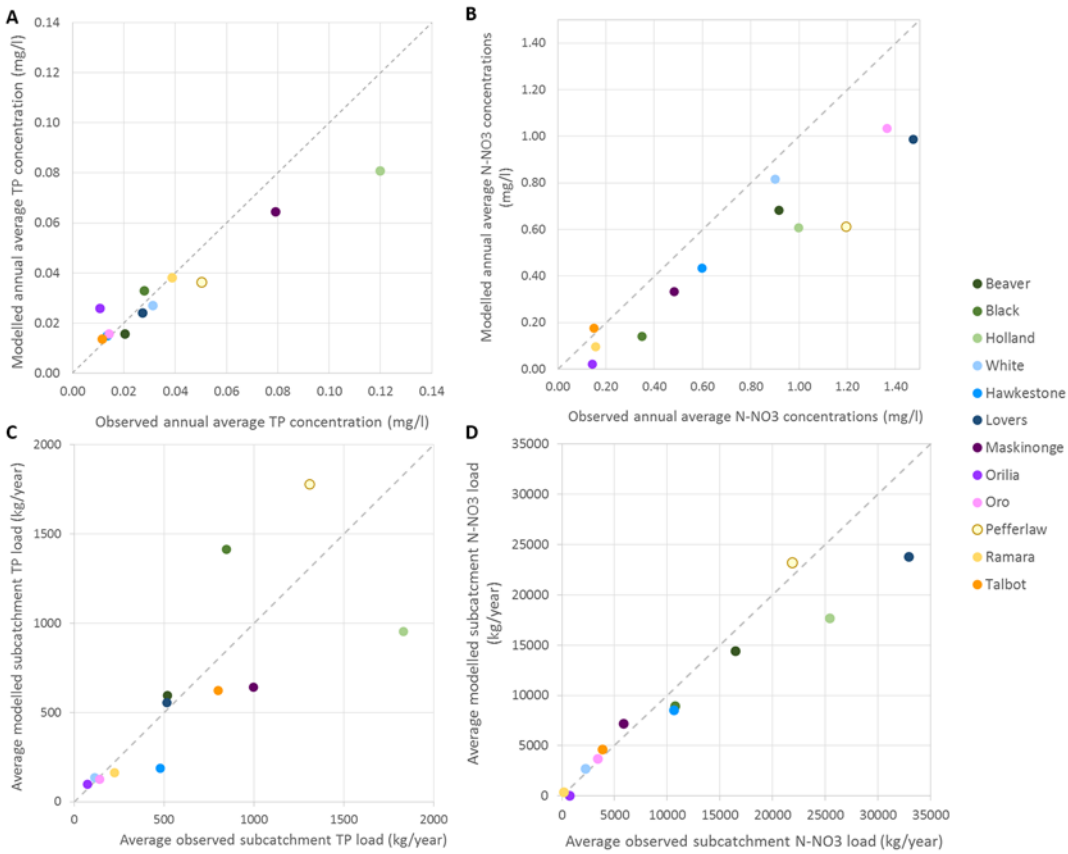

Fig. 5. Representation of model performance by catchment A) TP concentration; B) N-NO_3 concentration; C) TP load; D) N-NO_3 load.

only 12.8μg/l. In basins K42 and C9, model predictions were slightly less accurate at the annual scale, though associations were generally still good. Exceptions include Chl-*a* in basin K42 (R^2 reduced to 0.17) and N-NO_3 in basin C9 (R^2 reduced to 0.14). The RMSE associated with these models remained low, however, and comparable to values obtained at other time scales.

Model performance was validated at a daily timescale, during the period April 20th to June 1st 2016, when the Lake basins monitoring

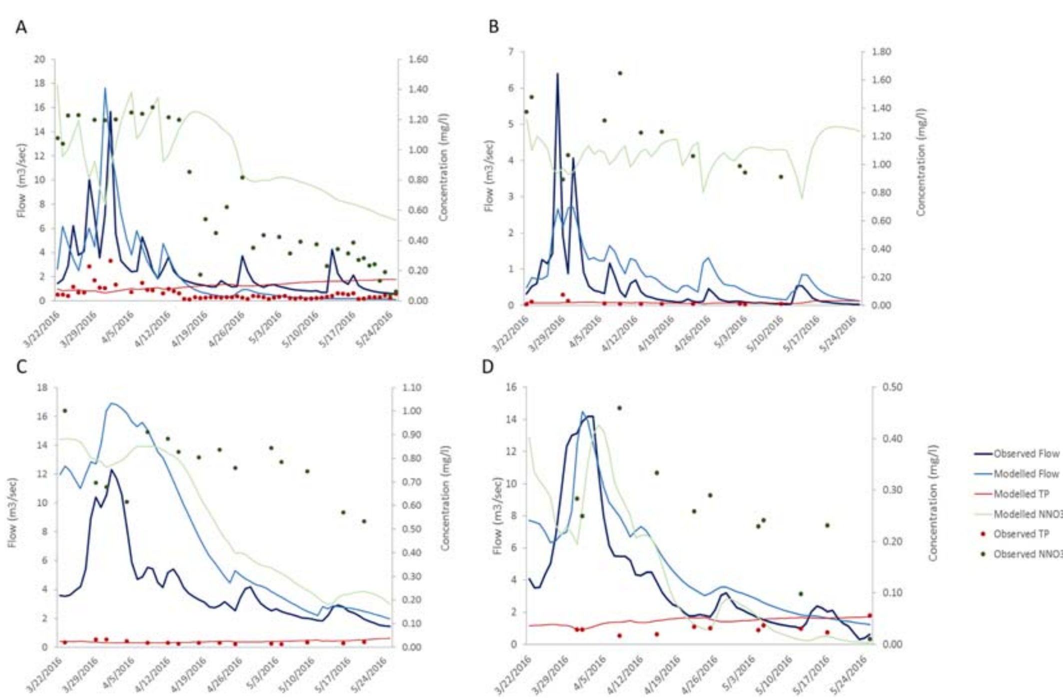

Fig. 6. Modelled and observed flow, N-NO_3 and TP concentrations during the primary spring melt period within A) Holland B) Oro C) Pefferlaw and D) Black.

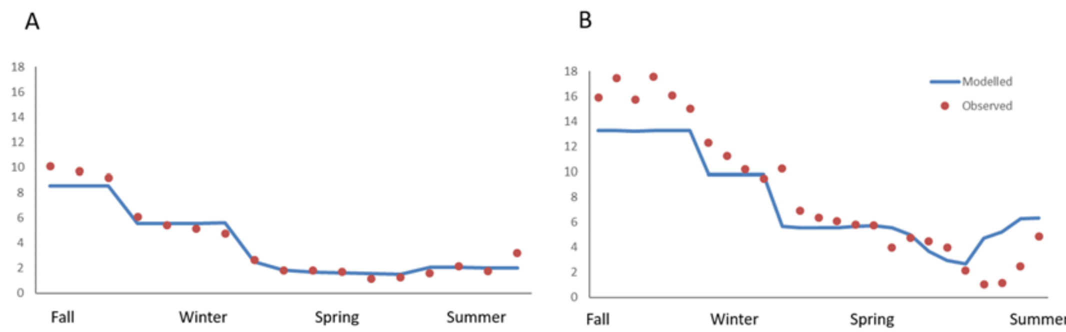

Fig. 7. SiO_2 model fit (daily) across two sub-catchments of Simcoe with contrasting soil types; A) Ramara (60% clay; R^2 0.97) and B) Orillia (6% Clay; R^2 0.87).

were conducted at a high frequency (Table 2). Daily temperatures and dissolved oxygen concentrations were simulated with an R2 of >0.93 and >0.5 in all basins respectively. Model performance of N-NO_3 and Chl-*a* were similar at the daily resolution to that obtained at seasonal and monthly. Lake model performance of TP concentrations was lower in basin K42 (R2 0.3), and RMSE was higher in all basins, where TP was over-predicted by the models during these events. Performance of SRP, however, maintained accuracy at this daily frequency.

Box plots of daily model output data were used to identify physical and chemical thresholds contributing to lake basin Chl-*a* and DO concentrations (Bowes et al., 2016) (Figs. 9 and 10). Concentrations of Chl-*a* were similar across a broad range of SRP and N-NO_3 conditions within all basins. Notably within basin K42, the median Chl-*a* concentrations were lower where SRP concentrations were higher. At both basins C9 and K42 all Chl-*a* concentrations above 2.5 μg/l occurred when tributary inflows were low (4 m^3/s in K42, and <8 m^3/s in basin C9). In basin E51, Chl-*a* concentrations were generally lower, and flows generally higher compared to other basins. Here all Chl-*a* concentrations above 1.8μg/l occurred when tributary inflows were below 20 m^3/s. In basin C9 the highest Chl-*a* concentrations occurred when temperature was between 11 and 23 °C, compared to basin K42 and E51 where high concentrations were found at low temperatures – ranging from 3 to 7 °C in K42, and 5-11 °C in E51.

DO concentrations of below 7 mg/l in the 5 m bottom zone are identified in Fig. 10 as 'critical events'. 7 mg/l is the ecologically relevant DO level at which adverse impacts upon cold water fish are initially observed (Garside, 1959; EPA, 1986; Evans, 2006). In basins K42 and C9 the critical threshold for DO was breached across a wide range of SRP and Chl-*a* concentrations. In basin E51 the threshold was only crossed where Chl-*a* concentrations were <0.6μg/l. Conversely, in all basins, DO critical events only occurred during periods of relatively low flow (<8 m^3/s in C9, <6 m^3/s in K42 and <25 m^3/s in E51). Similarly, the

Table 1
Driving variables and performance of SiO_2 model at various temporal scales.

Category	Variable	% impact on SiO_2 concentration	% SiO_2 variation explained by model		
			Daily	Seasonal	Annual
Clay < 1% (<10th percentile)	Discharge	0.953			
	SMD	0.188			
Clay 1–8% (10–40th percentile)	Discharge	−0.283			
	SMD	0.188			
Clay 8–42% (40th–70th percentile)	Discharge	0.805			
	SMD	0.249			
Clay > 42% (>70th percentile)	Discharge	0.744	60	80	90
	SMD	0.899			
Catchment area > 100 ha	Discharge	−0.729			
	Area	0.005			
Season	Spring	−4.067			
	Summer	−3.466			
	Autumn	3.098			
	Winter	0			

events only occurred during periods of higher temperature (21 °C in C9, and 15 °C in K42 and E51).

The wide range of DO values within each category indicates that the onset of critical events is likely driven by multiple-stressors. A more detailed insight into DO hysteresis can therefore be gained using a polynomial analysis of model results (SI3 and Fig. 12), which illustrate threshold interactions between multiple variables (Bowes et al., 2016).

The optimum temperature for algal growth at sites E51 and C9 is between 6 and 12 °C and 19–22 °C respectively (SI2). Temperatures required to reach specific Chl-*a* concentrations, and the amount of SRP required to produce algae are reduced where flows are lower (SI2 A,C,D, F). The optimum flow is <30 m^2 (E51) and <16 m^3/s (C9) (SI2 A, C). At site E51 where temperatures are >12 °C, higher Chl-*a* is associated with lower temperatures. The same effect is seen at site C9, above 19 °C (SI2 B, D). The optimum SRP concentrations for growth at site E51 are broad, ranging from 0.7–1.37. SRP concentrations above 1.37 μg/l are associated with reduced Chl-*a* concentrations. At site C9 much higher SRP is generally required for algal growth, between 2.4 and 2.6 μg/l. Generally at site C9, higher SRP is associated with greater Chl-*a* concentrations.

At site K42, the deepest basin, the multi-stressor relationships are more complex. The optimum temperature threshold for algal growth is between 10 and 18 °C and the optimum flow for algal growth is between 3 and 6 m^3/s (SI2 G). Above this flow threshold, in a similar response to sites E51 and C9, less Chl-*a* is found, even under higher temperatures (SI2, H). Conversely however, at this site extremely low flows are also associated with low Chl-*a* concentrations, even during high summer temperatures. There are two optimum SRP conditions for algal growth at this site; the first is <1.4 μg/l at low temperatures, and the second is >1.4 μg/l at high temperatures (SI2, H).

All polynomial analyses demonstrate significant relationships between variables. Although R^2 was low in basins E51 and K42, when analysis were run to include the effects of all three primary variables (temperature, flow and SRP) on Chl-*a*, the R^2 was much improved at 0.5 (E51 and C9), and 0.73 (K42).

Fig. 11A, D and G demonstrate that the combined effects of temperature and flow consistently provide the greatest explanation for variability in DO concentrations ($R^2 > 0.9$) in all three lake basins. Under the impacts of temperature and flow, DO levels may only drop below 7 mg/l when temperatures are above 17 °C (E51), 20 °C (K42), or 25 °C (site C9). Lower DO levels may be reached where flow is <6 m^3/s (E51 and K42), or 17 m^3/s (C9). The contour plots demonstrate how the 7 mg/l DO level can be reached across a broad range of Chl-*a* concentrations at sites E51 and C9 (Fig. 11B, E). At both sites higher Chl-*a* concentrations are associated with higher DO concentrations, once Chl-*a* reaches a critical mass (>0.5 μg/l in E51, and 2 μg/l in C9). At both sites, low flows are associated with low DO.

At site K42 again the relationships are more complex. Similar to other basins, DO events may occur across a wide range of Chl-*a* concentrations, and lower flows. At Chl-*a* concentrations <2 μg/l, DO is expected to be lower where flows are low and Chl-*a* is high (Fig. 11I). Where

Table 2
PROTECH model performance during the period 2010–2016. RMSE is reported in °C for temperature, mg/l for DO, and μg/l for N-NO_3, TP and Chl-*a*. Daily (event) performance is assessed during the period 20th April–1st June, when higher frequency monitoring data was available. SRP observed data has not been directly measured in the lake since 2008; observed SRP concentrations were calculated as a portion of TP using seasonal and annual correction factors, obtained from historic observed data. All calibrations are reported from the euphotic zone, with the exception of dissolved oxygen, where outputs are derived from the 5 m bottom zone of each basin.

Variable	Basin	R^2				RMSE			
		Seasonal	Monthly	Annual	Daily (event)	Seasonal	Monthly	Annual	Daily (event)
Temperature	C9	0.93	0.96	0.96	0.96	2.1	1.5	4.2	2.4
	K42	0.99	0.94	0.93	0.99	2.7	2.5	5.5	2.1
	E51	0.91	0.87	0.95	0.93	2.5	2.5	4.9	3.2
DO	C9	0.31	0.88	0.99	0.75	0.4	0.8	1.6	0.5
	K42	0.74	0.88	0.92	0.50	1.5	1.9	1.6	0.6
	E51	0.90	0.87	0.8	0.51	0.6	0.9	1.0	0.7
N-NO_3	C9	0.81	0.58	0.14	0.97	28.3	27.4	33.7	93.1
	K42	0.81	0.57	0.69	0.21	22.3	20.5	24.6	55.2
	E51	0.98	0.89	0.2	0.59	10.0	10.4	12.8	8.5
TP	C9	0.57	0.22	0.31	0.2	8.6	9.8	5.3	23.7
	K42	0.88	0.92	0.40	0.3	4.4	3.4	6.3	12.9
	E51	0.37	0.45	0.71	0.22	2.6	3.1	1.7	8.7
SRP	C9	0.57	0.18	0.38	0.74	0.5	0.6	0.3	0.7
	K42	0.88	0.92	0.40	0.30	0.4	0.3	0.5	0.7
	E51	0.37	0.45	0.71	0.37	0.2	0.2	0.1	0.4
Chl-*a*	C9	0.52	0.46	0.38	0.1	0.2	0.3	0.3	0.9
	K42	0.42	0.53	0.17	0.31	0.2	0.4	0.2	1.7
	E51	0.15	0.42	0.33	0.46	0.3	0.4	0.2	0.5

Chl-*a* concentrations >2 μg/l, lower DO is associated with lower Chl-*a* and higher flows. Importantly however, converse to other sites, at temperatures above 10 °C, higher Chl-*a* concentrations are associated with lower DO concentrations (Fig. 11H). Below this threshold the Chl-*a*:DO relationship is similar to other sites, where high Chl-*a* is associated with lower temperatures.

As suggested by Bowes et al. (2016), a timeseries analysis (Fig. 12) was used to determine the feasibility of the calculated multi-stressor thresholds. DO critical events during the modelling period were identified, and conditions under which they occurred compared to the thresholds determined. In basin E51, incidences of high temperature and low flow can account for all instances where lake DO concentrations dropped below 7 mg/l (referred to as DO7) (Fig. 12). During these events, Chl-*a* is consistently below 0.5 μg/l. During other periods where both flow and temperature are within the threshold to create DO7 conditions, Chl-*a* is consistently above the 0.5 μg/l threshold, and DO7 does not occur. Similarly in basin C9, the majority of DO7 events can be attributed to temperature and flow conditions. Flow is always below $17 m^3/s$ when DO7 occurs, although events a-d do occur below the predicted threshold for temperature. In most instances of DO7, Chl-*a* is below 2 μg/l. Events b and d occurred under higher Chl-*a* concentrations (2.5 and 3 μg/l), but only fell marginally below the 7 mg/l DO threshold. In basin K42 again the majority of DO7 events occurred through the effects of temperature and flow alone. Events a-c however can only be explained through additional impacts of Chl-*a* which acts to reduce the temperature threshold at which DO will reach 7 mg/l.

Importantly in all three basins, both modelled and observed DOD7 events generally occurred when values of driving variables (monitored and observed) fell within the calculated threshold values; supporting the results obtained from the multi-stressor analyses. The timing of DO7 events in Fig. 12 support the thresholds calculated through the polynomial analyses. Importantly, all three timeseries indicate that without the presence of Chl-*a*, DO7 events would continue to occur during hot summers and extreme low flow events.

4. Discussion

4.1. Model performance and uncertainty

All feeder models (INCA-N, INCA-P and Silica) performed well in simulating both long term historical trends (i.e. the weekly and bi-weekly monitoring data), and short term 'event' processes (i.e. the daily monitoring data). The similarity in performance between models applied to catchments of different soil types gives confidence in the simulations performed by the PERSIST-INCA model chain during extreme events across the range of catchment conditions presented by the Simcoe watershed, demonstrating that roughly equal confidence can be had in all regions. Based upon these simulations, the lake model PROTECH was able to accurately represent daily DO concentrations within the three major basins of Lake Simcoe, at multiple spatial and temporal resolutions.

Model and parameter uncertainty are inherent in any study involving water quality models; in general, the greatest sources of uncertainty tend to lie within the most sensitive but poorly characterised (or unmeasured) conditions (Wade et al., 2001). It is true that the INCA suite of models is complex, with many parameters needing careful calibration (Jackson-Blake et al., 2017). Complex models can be seen as being at a greater risk of equifinality, i.e. producing the same output from multiple combinations of different parameter values. However, model predictions are generally only sensitive to a few of those parameters and use of simplified model structures does not necessarily remove this issue (Futter et al., 2015). Indeed, in catchments with high spatial variance in soil structure (and hence, hydrology and resultant nutrient dynamics) like the Simcoe basin, the added complexity offered by the INCA models is an advantage, enabling the user to match model processes more closely to sub-catchment conditions. The assessment of spatial variance in management effectiveness, which is the ultimate aim of this tool, would not be possible using more simplistic catchment models.

Where a chain of models is used, uncertainties can be exacerbated as they "feed forward". It is for this reason that high temporal resolution of monitoring was conducted in both the river and lake during the previously un-monitored snowmelt period. The high calibration performance of the PROTECH model in simulating DO, TP and temperature, during 2016 daily events gives confidence in the accuracy of the linked model chain. It should be noted however that whilst flow and TP concentrations were well represented by the catchment models during this key hydrochemical event, N-NO_3 was generally under-predicted. As a result, N-NO_3 outputs to the lake during snow-melt should be interpreted with more caution. The additional monitoring data enabled assessments of PROTECH seasonal and monthly performances, at a basin scale, which would not otherwise have been possible. PROTECH

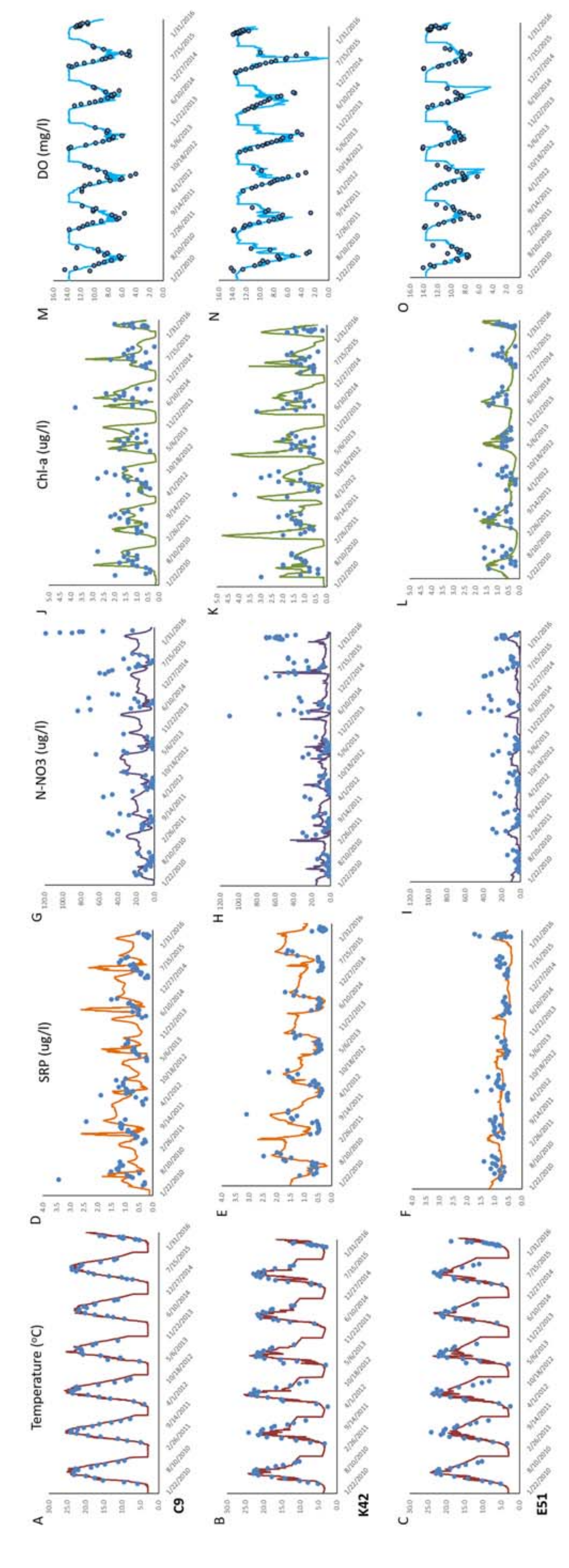

Fig. 8. PROTECH calibration outputs over the baseline period 2010–2016 (solid lines represent PROTECH simulation; dots represent observed data).

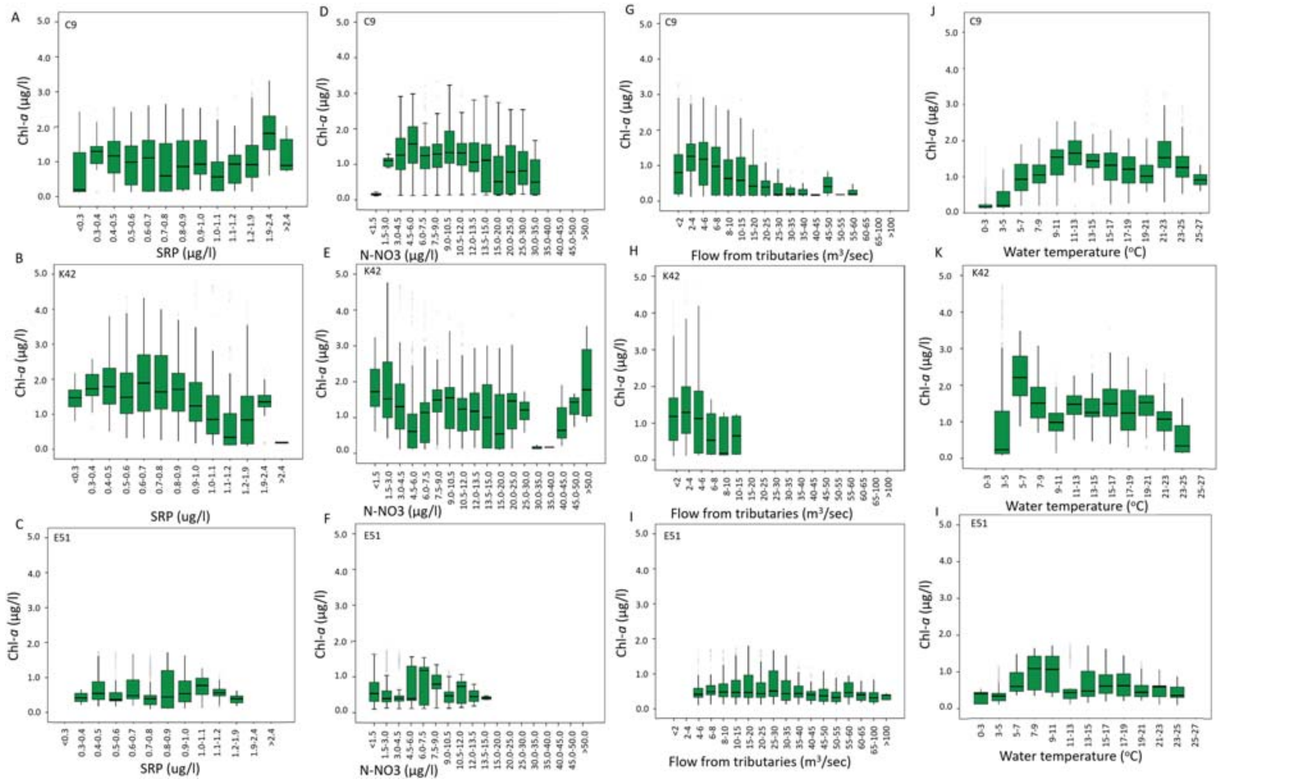

Fig. 9. Boxplots of chlorophyll concentrations in each of the major Simcoe basins, under varying conditions of SRP, N-NO_3, flow and water temperature.

performed well at both monthly and seasonal scales, across all parameters, although model performance was slightly poorer for Chl-*a* at an annual scale. This could relate to INCA model error in N-NO_3 outputs.

The joining of INCA and PROTECH provided a variety of benefits, primarily that both models operate at the same timescale, with the INCA suite providing the outputs required to drive PROTECH; making for an

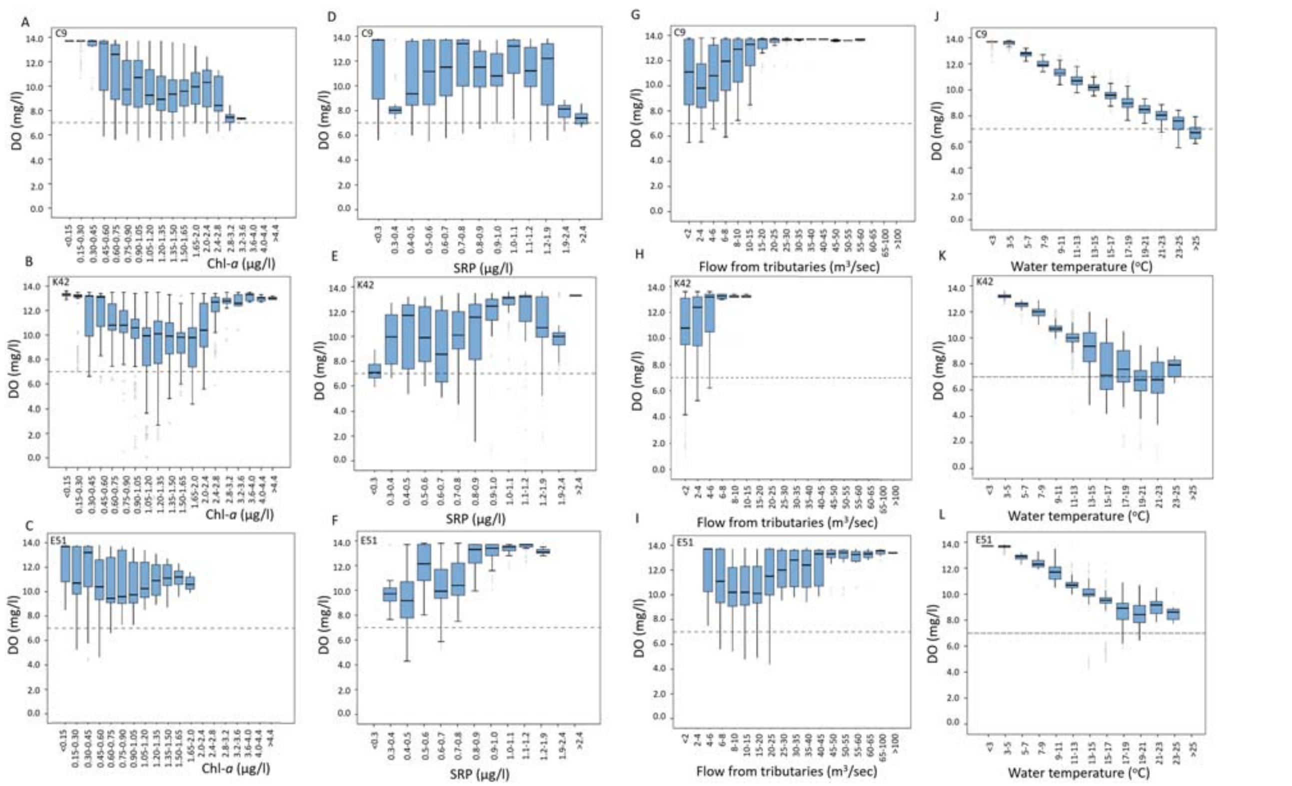

Fig. 10. Boxplots of lake DO concentrations in each of the major Simcoe basins, under varying conditions of chlorophyll, SRP, flow and water temperature. Dashed line indicates 7 mg/l DO concentration threshold.

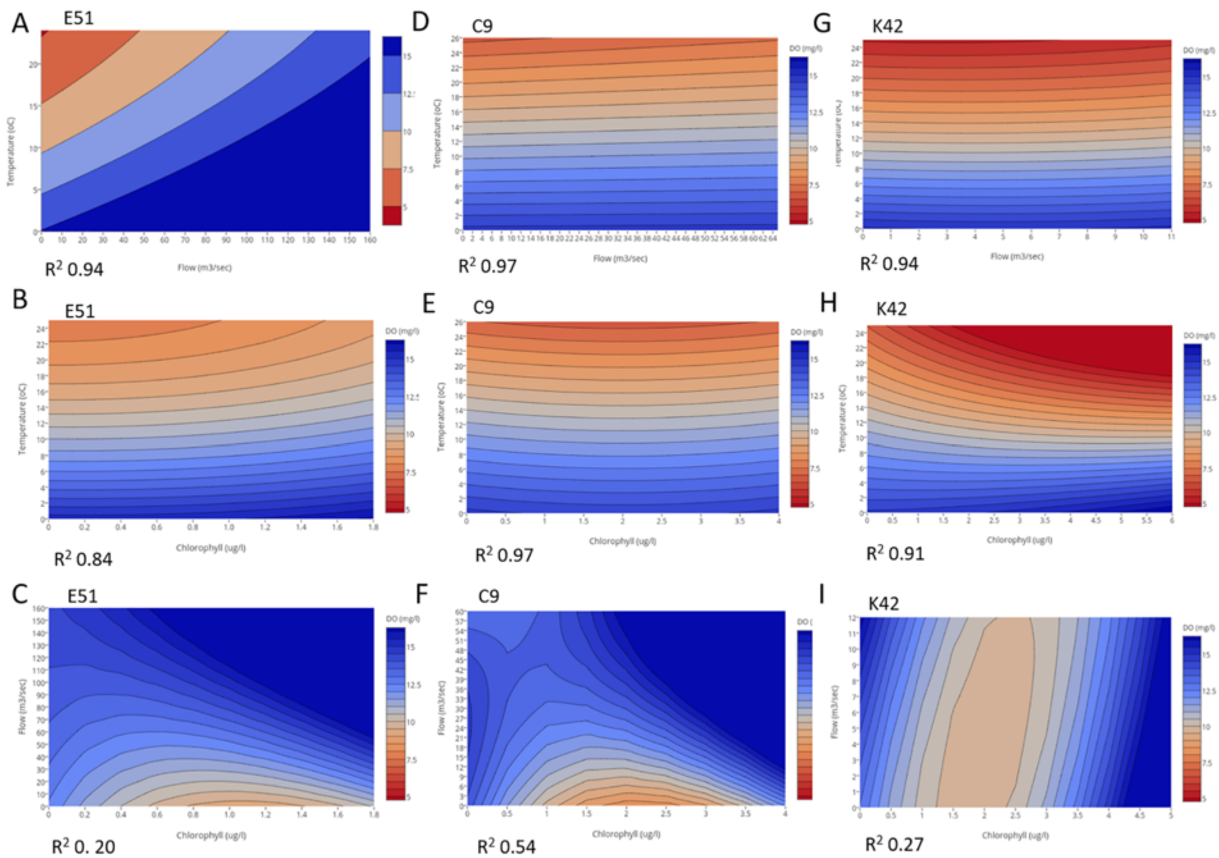

Fig. 11. Contour plots of polynomial analyses between DO concentrations simulated by PROTECH and a range of potential driving variables, including temperature and flow; temperature and chlorophyll-*a*, and flow and chlorophyll-*a*.

ideal model chain. In addition INCA is semi-distributed, with the capacity to model process interactions within and between an extensive number of tributaries and catchments, providing the ability to compare performances across different landuses, soil types and stream network densities. Although PROTECH is more spatially limited, three linked PROTECH models were used in this study. Lake monitoring points were chosen towards the mouth of each basin so as to limit any feed-forward errors between basins, however this does result in lake shoreline conditions being under-represented. For example, higher Chl-*a* concentrations and phytoplankton biomass have been found near the shoreline of Cooks bay, compared to site C9 (Eimers et al., 2005), and greater numbers of zebra mussels are generally seen in at or near the shoreline regions of the lake (Schwalb et al., 2013).

The precautionary principle (Walker et al., 2003) indicates that it could be wise to accept uncertainties in assessments where adverse impacts to the environment are involved. Considering the success of the linked model's performance, this principle supports the use of the model chain in analysing physical, chemical and biological hysteresis within the lake basins, and its use in offering a meaningful insight into potential responses to land-use management efforts.

4.2. Model simulations

4.2.1. Chlorophyll-a

In both basins E51 and K42, the high concentrations of Chl-*a* simulated at low temperatures reflects the occurrence of spring phytoplankton blooms, taking place during or shortly after the break-up of lake ice. The multi-stressor analysis demonstrated marked differences in optimum algal growing conditions in the deeper K42 basin between spring and summer periods, of a negative association with SRP (<1.4 μg/l) during low temperatures, and a positive correlation with SRP (>1.4 μg/l) during higher temperatures. This is suggestive of the occurrence of two independent bloom events (Ye et al., 2007). The negative association between Chl-*a* and SRP in cooler temperatures could be indicative of periods where algal growth control SRP (Bowes et al., 2016). These findings are consistent with those of Weyhenmeyer (2001) who demonstrated that algal blooms are common upon initial ice break-up in early spring, when growth is limited not by nutrient concentrations, but by light and temperature conditions. As algal growth persists, and waters become progressively warmer, nutrient concentrations subsequently decline until a point is reached whereby algal growth is limited by nutrient availability (Ye et al., 2007). This nutrient-limitation period is demonstrated by the INCA-PROTECH model through a positive association between Chl-*a* and SRP concentrations in warmer waters in basins K42 and C9.

The association between low tributary inflows and high Chl-*a* concentrations in all basins are likely due to longer residence times associated with reduced inflow, a more stable thermocline, and warmer surface waters (Straskraba and Hocking, 2002). The relationship is complicated by the progressively reduced impact that temperature has upon algal growth under increasing temperatures, such that algae becomes limited by alternative driving factors in warmer waters (Vrede, 2005), e.g. by the aforementioned summer declines in SRP concentrations in basin C9 and K42. This reduced impact of temperature upon Chl-*a* under warmer conditions could explain why higher Chl-*a* is associated with cooler water temperatures above a temperature threshold of 12 °C and 19 °C respectively in basins E51 and C9. In addition previous studies have indicated that algal growth can have a positive feedback effect on the thermal structure of the lake (Rinke et al., 2010), caused by a self-shading effect of the algae, which results in greater light-extinction and restricts water temperatures (Schindler et al., 1996). Although this is a likely additional explanation for the relationship in the observed timeseries analysis, as PROTECH's algae light-extinction coefficient

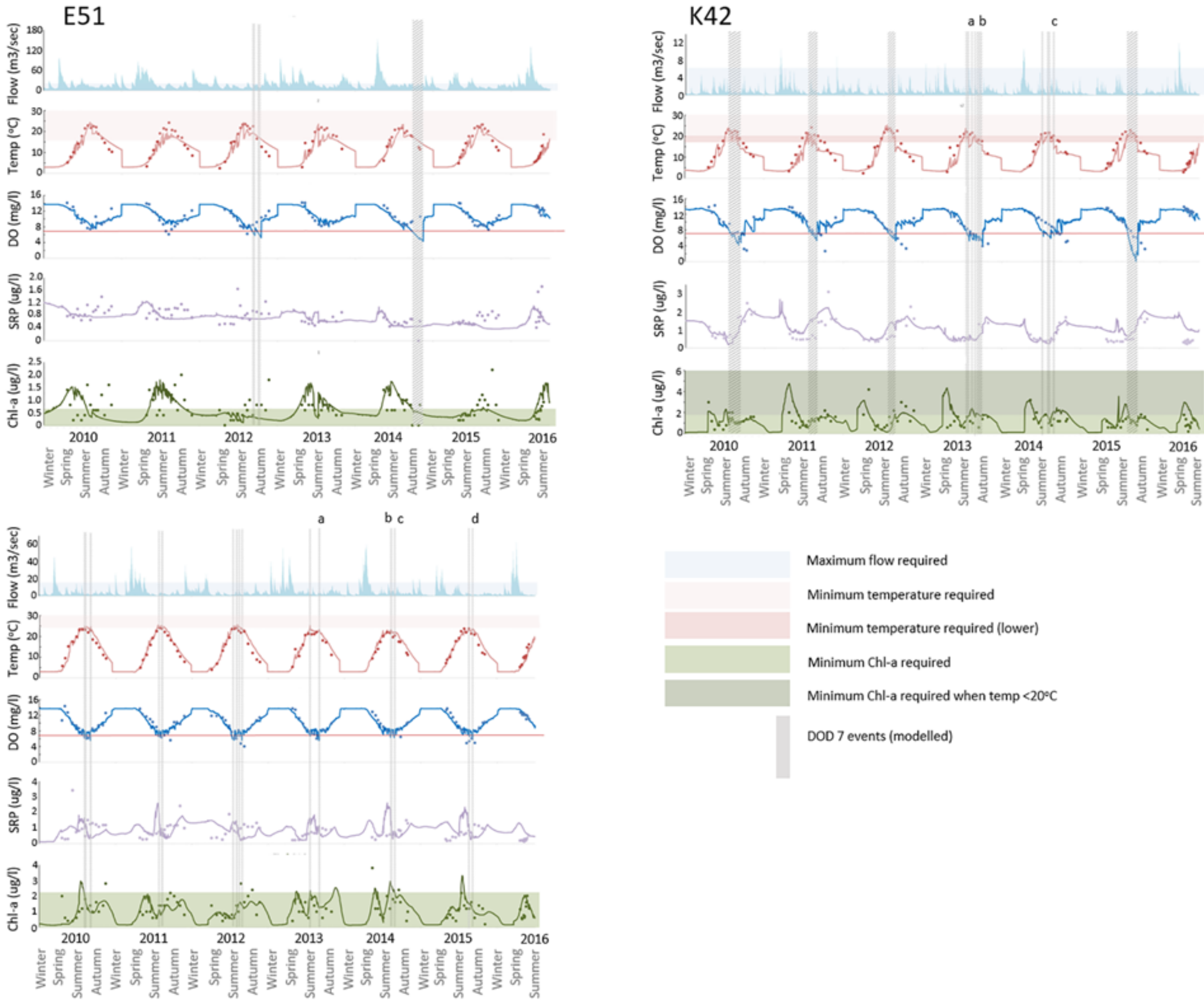

Fig. 12. time series of observed and modelled data, indicating that DO7 events accounted for multistressor thresholds. (Continuous lines represent PROTECH model outputs, points represent observed data).

does not affect heat energy within the model, a self-shading mechanism cannot explain the DO response simulated by the model.

4.2.2. Dissolved oxygen

Lake DO concentrations are dependent upon a variety of conditions and processes. First, oxygen is more soluble in cooler water and thus as waters warm DO concentrations decrease. Additionally processes supply and use oxygen to and from the lake. Sources include reaeration from the atmosphere, production from photosynthesis, and from incoming tributaries; and losses include respiration either by plants or by bacteria during breakdown of organic matter (biochemical oxygen demand), and use by river bed sediments (sediment oxygen demand) (Cox, 2002). In a stratified lake, if the balance of losses exceeds the inputs within any particular thermal layer, a decline in lake DO concentrations will occur in that zone.

Considering the variety of Chl-*a* concentrations across which DO7 events occurred, analyses indicated that losses related to algal growth were not the primary driver of DO7 events within the 5 m bottom zone of any basin within Lake Simcoe. Conversely, the small cluster of temperature and tributary inflow conditions across which events were projected suggested these variables have a more significant influence. As DO concentrations did not consistently fall below 7 mg/l across thresholds determined for any one variable in isolation, a multi-stressor effect is likely. For instance, the polynomial analysis demonstrated that in order for a DO7 event to occur at site K42 or E51, flow must be below 6 m^3/s and temperature > 20 °C or 17 °C respectively; similarly at site C9 flow must be lower than 17m^3/s and temperature > 25 °C. In addition to the effect of warmer waters holding lower DO concentrations, the impact of reduced inflows is two-fold. Firstly, lower flows increase the residence time of water in the hypolimnion, which may increase the sediment oxygen demand (Nakamura and Stefan, 1994). This leads to lower DO concentrations at equivalent temperatures. Secondly, these lower flow rates and higher residence times could reduce the epilimnion thickness, and increase surface warming (Rimmer et al., 2011). This results in an increase in stability of the thermal profile (Straskraba and Hocking, 2002) which becomes more resistant to wind-induced mixing. At extremely low flows these warmer temperatures can extend into the hypolimnion, reducing the DO content held, and result in DO7 events.

At the shallower sites E51 and C9, Chl-*a* and DO are positively associated above a critical concentration of 0.5 and 2 μg/l Chl-*a* respectively. The positive association between Chl-*a* and DO is attributed in part to the reduced impact of temperature as a driving variable in warmer waters; i.e. in summer higher Chl-*a* concentrations were identified as occurring in lower water temperatures, which hold more DO. Importantly however the threshold analyses indicated that declines in DO are inhibited when Chl-*a* concentrations are above a particular threshold. Oxygen gains from photosynthesis during summer usually exceed losses from decomposition and respiration (Chapra, 1997), and these results suggest that in these shallow, more weakly stratified basins, O_2 supplied to the water column through photosynthesis under high algal growth rates limits the decline of DO concentrations caused by physical conditions.

At the deeper, more stratified site K42, which was observed to experience a greater number of DO7 events, effects of reaeration from photosynthesis are unsurprisingly not observed within the 5 m bottom zone. Results indicate that in fact during summer, algal growth leads to oxygen losses as a result of enhanced BOD, which adds to the DO depletion effect of the physical drivers. When water temperatures are >10 °C, Chl-*a* concentrations are negatively associated with DO concentrations, which is indicative of an increase in BOD, through bacterial uptake of oxygen from decaying organic matter (Stefan and Fang, 1994). The summer BOD effect is supported by the timeseries analysis (Fig. 12), where three of the DO7 events could not be explained solely by temperature and flow interactions. Although at this site, similar to in other basins, there is a critical Chl-*a* threshold (2 μg/l) above which DO is positively associated with Chl-*a* and flow, the reason for this threshold is quite different than at the shallower sites as here these high Chl-*a* concentrations occur predominantly in spring, and this association reflects the manifestation of spring algal blooms, which occur in cooler, oxygen-rich waters.

Importantly, the multi-stressor relationships and time-series analysis indicate that in all basins, concentrations of DO could continue to drop below 7 mg/l critical levels, under high temperatures and extreme low flows; irrespective of improvements in Chl-*a* concentrations. These findings have implications for future land management, especially when considering the impacts of climate change. Under potential future increases in temperatures and changes in precipitation, lake health could become increasingly dependent upon flow volume and water temperature. Where there is a current focus on reducing nutrient loads to Lake Simcoe, emphasis might perhaps be shifted to additionally preserving tributary flow volumes, and reducing only nutrient concentrations.

5. Conclusion

The process-based catchment models INCA-N and INCA-P formed an effective chain with the lake model PROTECH, to accurately simulate monitored trends in water quality, both across a long-term historic annual timescale (1985–2016), and at a high resolution daily event-basis.

In each basin of lake Simcoe DO7 events were identified to occur at different thresholds of various physical and biological drivers. In each basin, although Chl-*a* concentrations were at times limited by phosphorus availability, physical conditions such as tributary inflow quantities and temperature had additional important impacts on algal growth. Chl-*a* did not have the expected impact on lake DO. In all basins the majority of DO7 events could be explained by the interactions between high temperatures and low flows. Within the shallow basins E51 and C9, the impacts of these physical drivers were on occasion reduced by contributions of O_2 to the lake from photosynthesis, which exceeded biological oxygen demand in summer when algal growth rates were sufficient. The effects of photosynthesis were less dominant in the deeper more strongly stratified K42 basin, where instead algal growth enhanced the biochemical oxygen demand, and added to the DO decline driven by physical conditions. Importantly, the analysis demonstrates that irrespective of Chl-*a*, basin DO concentrations could still fall below critical thresholds during extreme low flows, and at high temperatures, suggesting that warmer drier summers will reduce the health (DO concentrations) of Lake Simcoe.

In summary the INCA-PROTECH model chain provides a unique combination of large spatial distribution, with the option for high temporal frequency. With a direct transition between catchment model outputs to lake model inputs, this effective model chain could in future be used to simulate success of management strategies, and the potential basin responses to changes in landuse and climate. Such applications could help to provide additional process understanding of the hysteresis of flow, nutrients, phytoplankton and DO concentration within rivers, bays and lakes across the world.

Acknowledgements

This study was funded by the Environment Canada Lake Simcoe Georgian Bay Clean Up Fund (grant number: GCXE16R150). Trent University would like to thank the volunteers Mitch Hall, Jacob Bothen and Joel Winer, who provided help during field data collection. Thanks also for the INCA-N modelling support provided by Dr. Stephen Oni and for the outstanding work performed by the Trent University Field and Lab Technician, Dave Woods. ISCO samplers were loaned by Professor Catherine Eimers of Trent University, for which we are very grateful. Historic data was kindly provided by the Lake Simcoe Region Conservation Authority (Lance Aspden and Eavan O'Connor) and the Ministry of Environment and Climate Change (Dr Joelle Young, Dr. Michelle Palmer, Claire Holten and Dr. Hamdi Jarjanazi, and Dr. Jennifer Winter). Identification of phytoplankton species was carried out by Elaine Carney. Finally thank you also to Professor Martyn Futter (Swedish University of Agricultural Sciences), Professor Paul Whitehead (Oxford University), Professor Lew Molot (York University) and Dan Butterfield for their invaluable insights into model operations and systems processes.

Appendix A. Supplementary data

Supplementary data to this article can be found online at https://doi.org/10.1016/j.scitotenv.2017.12.052.

References

Agriculture and Agri-Food Canada, 2010. Detailed Soil Survey (DSS) Compilations. Available online at. http://sis.agr.gc.ca/cansis/nsdb/dss/v3/index.html.

Bell, V.A., George, D.G., Moore, R.G., Parker, J., 2006. Using a 1-D mixing model to simulate the vertical flux of heat and oxygen in a lake subject to episodic mixing. Ecol. Model. 1980, 41–54.

Bowes, M.J., Lowenthal, M., Read, D.S., Hutchins, M.G., Prudhomme, C., Armstrong, L.K., Harman, S.A., Wickham, H.D., Gozzard, E., Carvalho, L., 2016. Identifying multiple stressor controls on phytoplankton dynamics in the River Thames (UK) using high-frequency water quality data. Sci. Total Environ. 1489–1499.

Breitburg, D.L., Loher, T., Pacey, C.A., Gerstein, A., 1997. Varying effects of low dissolved oxygen on trophic interactions in an estuarine food web. Ecol. Monogr. 67 (4), 489–507.

Burns, N.M., Rockwell, D.C., Bertram, P.E., Dolan, D.M., Ciborowski, J.J.H., 2005. Trends in temperature, secchi depth and dissolved oxygen depletion rates in the central basin of Lake Erie, 1983–2002. J. Great Lakes Res. 31 (Supplement 2), 35–49.

Canadian Hydrographic Service, 1957. Depth Sounding Field Data, Scale 1:36,000 (Digitised by the Ontario Ministry of Natural Resources).

Casson, N.J., Eimers, M.C., Buttle, JM., 2010. The contribution of rain-on-snow events to nitrate export in the forested landscape of south-central Ontario, Canada. Hydrol. Process. 24, 1985–1993.

Chapra, S.C., 1997. Surface water quality modelling. McGraw-Hill International Editions.

Conley, D.J., 2000. Biogeochemical nutrient cycles and nutrient management strategies. Hydrobiologia 410, 87–96.

Cooper, G.P., Washburn, G.M., 1949. Relation of dissolved oxygen to winter mortality of fish in Michigan lakes. Trans. Am. Fish. Soc. 76 (1), 22–33.

Cox, B.A., 2002. Dynamic Modelling of Dissolved Oxygen. A Case-study for the River Thames. (A thesis submitted for the degree of Doctor of philosophy). Department of Geography. University of Reading.

Crossman, J., Futter, M.N., Whitehead, P.G., Stainsby, E., Baulch, H.M., Jin, L., Oni, S.K., Wilby, R.L., Dillon, P.J., 2014. Flow pathways and nutrient transport mechanisms drive hydrochemical sensitivity to climate change across catchments with different geology and topography. Hydrol. Earth Syst. Sci. 18, 5125–5148.

Crossman, J., Futter, M.N., Palmer, M., Whitehead, P.G., Baulch, H.M., Woods, D., Jin, L., Oni, S.K., Dillon, P.J., 2016. The effectiveness and resilience of phosphorus management practices in the Lake Simcoe watershed, Ontario, Canada. J. Geophys. Res. Biogeosci. 121, 2390–2409.

Diaz, R.J., 2001. Overview of hypoxia around the world. J. Environ. Qual. 30, 275–281.

Dittrich, M., Chesnyuk, A., Gudimov, A., McCulloch, J., Quazi, S., Young, J., Winter, J., Stainsby, E., Arhondistsis, G., 2013. Phosphorus retention in a mesotrophic lake under transient loading conditions: insights from a sediment phosphorus binding study. Water Res. 47, 1433–1447.

Eimers, M.C., Winter, J.G., Scheider, W.A., Watmough, S.A., Nicholls, K.H., 2005. Recent changes and patterns in the water chemistry of Lake Simcoe. J. Great Lakes Res. 31, 322–332.

Elliott, J.A., Bell, V.A., 2011. Predicting the potential long-term influence of climate change on vendace (*Coregonus albula*) habitat in Bassenthwaite Lake, U.K. Freshw. Biol. 56, 395–405.

Elliott, J.A., Persson, I., Thackeray, S.J., Blenckner, T., 2007. Phytoplankton modelling of Lake Erken, Sweden by linking the models PROBE and PROTECH. Ecol. Model. 202, 421–426.
Elliott, J.A., Irish, A.E., Reynolds, C., 2010. Modelling phytoplankton dynamics in fresh waters: affirmation of the PROTECH approach to simulation. Fr. Rev. 3, 75–96.
EPA, 1986. Ambient Aquatic Life Water Quality Criteria for Dissolved Oxygen (Freshwater). Office of Water Regulations and Standards Criteria and Standards Division, Washington DC (EPA 440/5-86-002).
Evans, D.O., 2006. Effects of Lake Hypoxia on Scope-for-Activity of Lake Trout: Defining a New Dissolved Oxygen Criterion for Protection of Lake Trout Habitat. Aquatic Research and Development Section, Applied Research and Development Branch. Ministry of Natural Resources.
Evans, D.O., Nicholls, K.H., Allen, Y.G., McMurtry, M.J., 1996. Historical land use, phosphorus loading and loss of fish habitat in Lake Simcoe, Canada. Can. J. Fish. Aquat. Sci. 53 (Suppl.1), 194–218.
Fournier, R.E., Morrison, I.K., Hopkin, A.A., 1994. Short range variability of soil chemistry in three acidic soils in Ontario, Canada. Commun. Soil Sci. Plant Anal. 25 (17–18), 3069–3082.
Futter, M.N., Erlandsson, M.A., Butterfield, D., Whitehead, P.G., Oni, S.K., Wade, A.J., 2014. PERSiST: a flexible rainfall-runoff modelling toolkit for use with the INCA family of models. Hydrol. Earth Syst. Sci. 18, 855–873.
Futter, M.N., Whitehead, P.G., Sarkar, S., Rodda, H., Crossman, J., 2015. Rainfall runoff modelling of the Upper Ganga and Brahamaputra basins using PERSiST. Environ. Sci. Proc. Impacts 17, 1070–1081.
Garside, E.T., 1959. Some effects of oxygen in relation to temperature on the development of lake trout embryos. Can. J. Zool. 37, 689–698.
Imberger, J., 1985. Thermal characteristics of standing waters: an illustration of dynamic processes. Hydrobiologia 15, 7–29.
Jackson-Blake, L.A., Sample, J.E., Wade, A., Helliwell, R.C., Skeffington, R., 2017. Are current dynamic water quality models too complex? A comparison of a new parsimonious phosphorus model, SimplyP, ad INCA-P. Water Resour. Res. https://doi.org/10.1002/2016WR020132.
Janhurst, S., 1998. Performance report: general chemistry and microbiology analyses section. Ontario Ministry of Environment Report. Queens Printer for Ontario, Ontario, Canada.
Kaas, H., Møhlenberg, F., Josefson, A., Rasmussen, B., Krause-Jensen, D., Jensen, H.S., Svendsen, L., Windolf, J., Middelboe, A.L., Sand-Jensen, K., Pedersen, M.F., 1996. Marine Områder. Danske Fjorde—Status over Miljøstand, årsagssammenhænge og udvikling. Ministry of the Environment and Energy, National Environmental Research Institute (No. 179). Report.
Koski–Vähälä, J., 2001. Role of resuspension and silicate in internal phosphorus loading. Dissertation in Limnology. Dep. of Limnology and Environmental Protection, Dep. of Applied Chemistry and Microbiology, Univ. of Helsinki, Helsinki.
Kramer, D.L., 1987. Dissolved oxygen and fish behaviour. Environ. Biol. Fish 18 (2), 81–92.
Lake Ice Analysis Group, 2012. Global Lake and River Ice Phenology. Data available online at. http://nsidc.org/data/docs/noaa/g01377_lake_river_ice/index.html.
Louis Berger Group Inc, 2010. Estimation of the phosphorus loadings to Lake Simcoe. The Louis Berger Group Inc, Washington DC.
MacLean, J.A., Eavans, D.O., Martin, N.B., Desjardin, R.L., 1981. Survival, growth, spawning distribution and movements of introduced and native trout (*Salvalinus namaycush*) in two inland Ontario Lakes. Can. J. Fish. Aquat. Sci. 38, 1685–1700.
May, L., Place, C., O'Malley, M., Spears, B., 2011. The Impacts of Phosphorus Inputs from Small Discharges on Designated Freshwater Sites (Final Report to Natural England and Broads Authority).
McMahon, R.F., 1991. Mollusca: ivalvia. In: Thorp, J.H., Covich, A.P. (Eds.), Ecology and Classification of North American Freshwater Invertebrates. Academic Press, San Diego (CA), pp. 315–399.
Nakamura, Y., Stefan, H.G., 1994. Effect of flow velocity on sediment oxygen demand: theory. J. Environ. Eng. 120 (5), 996–1016.
Neitsch, S.L., Arnold, J.G., Kiniry, J.R., Williams, J.R., 2011. Soil and Water Assessment Tool Theoretical Documentation Version 2009 (Agrilife Research and Extension).
Nicholls, K.H., 1997. A limnological basis for a Lake Simcoe phosphorus loading objective. Lake Reserv. Manag. 13 (3), 189–198.
O'Connor, E.M., Aspden, L., Winter, J.G., Lembcke, D., 2013. Optimisation of water quality sampling and load estimation modelling in the Lake Simcoe watershed: evaluations using a continuous phosphorus dataset. 2nd Biennial Lake Simcoe Science Forum.
OMAFRA, 2009. Ontario Ministry of Agriculture, Food and Rural Affairs: Agronomy guide for field crops. [Available at http://www.omafra.gov.on.ca/english/crops/pub811/1toc.htm] (last access 3 January 2014).
Oni, S.K., Futter, M.N., Molot, L.A., Dillon, P.J., 2014. Adjacent catchments with similar patterns of land use and climate have markedly different dissolved organic carbon concentration and runoff dynamics. Hydrol. Process. 28, 1436–1449.
Ontario Ministry of Natural Resources, 2007. Ecological Land Classification of Ontario (ELC). Available for download at. https://www.javacoeapp.lrc.gov.on.ca/geonetwork/srv/en/main.home, Accessed date: 15 January 2015.
Peltouvouri, T., 2006. Phosphorus in Agricultural Soils of Finland - Characterisation of Reserves and Retention in Mineral Soil Profiles, Pro Terra No. 26. (Academic Dissertation). Helsinki, University of Helsinki.
Provincial Groundwater Monitoring Network, 2012. Provincial Groundwater Monitoring Network Program: groundwater level data, groundwater chemistry data, and precipitation data, Ministry of Environment. Available at. https://www.javacoeapp.lrc.gov.on.ca/geonetwork/srv/en/metadata.
Ramwekellan, J., Gharabaghi, B., Winter, J.G., 2009. Application of weather radar in estimation of bulk atmospheric deposition of total phosphorus over Lake Simcoe. Can. Water Resour. J. 34, 37–60.
Rasmussen, J.B., Kalff, J., 1987. Empirical models for zoobenthic biomass in lakes. Can. J. Fish. Aquat. Sci. 44, 990–1001.
Reckhow, K.H., Norris, N.E., Budell, R.J., Di Toro, D.M., Galloway, J.N., Greening, H., 2011. Achieving nutrient and sediment reduction goals in the Chesapeake Bay: An evaluation of program strategies and implementation National Academic Press Washington DC.
Rimmer, A., Gal, G., Opher, T., Lechinsky, Y., Yacobi, Y.Z., 2011. Mechanisms of long-term variations in the thermal structure of a warm lake. Limnol. Oceanogr. 56 (3), 974–988.
Rinke, K., Yeates, P.S., Rothhaupt, K., 2010. A simulation study of the feedback of phytoplankton on thermal structure via light extinction. J. Freshw. Biol. 55, 1674–1693.
Schindler, D.W., et al., 1996. The effects of climatic warming on the properties of boreal lakes and streams at the Experimental Lakes Area, northwestern Ontario. Limnol. Oceanogr. 41, 1004–1017.
Scheider, W.A., Moss, J.J., Dillon, P.J., 1978. Measurement and uses of hydraulic and nutrient budgets. Lake Restoration, proceedings of a national conference, Minneapolis, Minnesota, USA 22-24 August.
Schwalb, A.N., Bouffard, D., Ozersky, T., Boegman, L., Smith, R.E.H., 2013. Impacts of hydrodynamics and benthic communities on phytoplankton distributions in a large, dreissnid-colonised lake (Lake Simcoe, Ontario, Canada). Inland Waters 3, 269–284.
Sharpley, A.N., Richards, R.P., Herron, S., Baker, D.B., 2012. Case study comparison between litigated and voluntary nutrient management strategies. J. Soil Water Conserv. 67, 149–193.
Smith, D.R., King, K.W., Willians, M.R., 2015. What is causing the harmful algal blooms in Lake Erie? J. Soil Water Conserv. 70 (2), 27–29.
Snodgrass, W.J., Holubeshen, J., 1992. Hypolimnetic oxygen dynamics in Lake Simcoe Part 3. Lake Simcoe Environmental Management Strategy Technical Committee. LSEMS Implementation Tech.Rep. No. Imp. B.15.
Soil Landscapes of Canada Working Group, 2010. Soil Landscapes of Canada version 3.2. Agriculture and Agri-Food Canada (digital map and database at 1:1 million scale).
Statistics Canada, 2011. Farm and operator data. Census of Agriculture.
Stefan, H.G., Fang, X., 1994. Dissolved oxygen model for regional lake analysis. Ecol. Model. 37–68.
Stephens, S.L.S., 2007. Optimising Agricultural and Urban Pollution Remediation Measures Using Watershed Modelling: Review, Calibration, Validation and Applications of the CANWET Model in the Lake Simcoe Watershed, Ontario, Canada. (MS thesis). Trent University, Trent.
Straskraba, M., Hocking, G., 2002. The effect of theoretical retention time on the hydrodynamics of deep river valley reservoirs. Int. Rev. Hydrobiol. 87 (1), 61–83.
Thornton, P.E., Thornton, M.M., Mayer, B.W., Wei, Y., Devarakonda, R., Vose, R.S., Cook, R.B., 2016. Daymet: Daily Surface Weather Data on a 1-km Grid for North America, Version 3. ORNL DAAC, Oak Ridge, Tennessee, USA. Accessed January 16, 2017. Time period: 1985-01-01 to 2015-12-31. https://doi.org/10.3334/ORNLDAAC/1328.
Väänänen, R., 2008. Phosphorus Retention in Forest Soils and the Functioning of Buffer Zones Used in Forestry. Dissertationes Forestales 60. Department of Forest Ecology, University of Helsinki, Helsinki, p. 42.
Vrede, K., 2005. Nutrient and temperature limitation of bacterioplankton growth in temperate lakes. Microb. Ecol. 49 (2), 245–256.
Wade, A.J., Hornberger, G.M., Whitehead, P.G., Jarvie, H.P., Flynn, N., 2001. On modelling the mechanisms that control in-stream phosphorus, macrophyte, and epiphyte dynamics: an assessment of a new model using general sensitivity analysis. Water Resour. Res. 37:2777–2792. https://doi.org/10.1029/2000WR000115.
Walker, W.E., Harremoës, P., Rotmans, J., Van Der Sluijs, J.P., Van Asselt, M.B.A., Janseen, P., Krayer Von Krauss, M.P., 2003. Defining uncertainty: a conceptual basis for uncertainty management in model-based decision support. Integr. Assess. 4 (1), 5–17.
Watson, S.B., Miller, C., Arhondistsis, G., Boyer, G.L., et al., 2016. The re-eutrophication of Lake Erie: harmful algal blooms and hypoxia. Harmful Algae 56, 44–66.
Weyhenmeyer, G.A., 2001. Warmer winters: are planktonic algal populations in Sweden's largest lakes affected? Ambio 30 (8), 565–572.
Winter, J.G., Eimers, M.C., Dillon, P.J., Scott, L.D., Scheider, W.A., Willox, C.C., 2007. Phosphorus inputs to Lake SImcoe from 1990 to 2003: Declines in tributary loads and observations on lake water quality. J. Great Lakes Res. 33 (2), 381–396.
Winter, J.G., Young, J.D., Landre, A., Stainsby, E., Jarjanzi, H., 2011. Changes in phytoplankton community composition of Lake Simcoe from 1980 to 2007 and relationships with multiple stressors. J. Great Lakes Res. 37, 63–71.
Ye, L., Han, X.Q., Xu, Y.Y., Cai, Q.H., 2007. Spatial analysis for spring bloom and nutrient limitation in Xiangxi bay of three Gorges Reservoir. Environ. Monit. Assess. 127 (1), 135–145.